Atmos. Chem. Phys. Discuss., doi:10.5194/acp-2016-567, 2016
Manuscript under review for journal Atmos. Chem. Phys.
Published: 25 July 2016

Atmospheric Chemistry and Physics Discussions

Development of a high-resolution emission inventory and its evaluation through air quality modeling for Jiangsu Province, China

Yaduan Zhou[1], Yu Zhao[1,2*], Pan Mao[1], Qiang Zhang[3], Jie Zhang[2,4], Liping Qiu[1], Yang Yang[1]

1. State Key Laboratory of Pollution Control & Resource Reuse and School of the Environment, Nanjing University, 163 Xianlin Ave., Nanjing, Jiangsu 210023, China

2. Jiangsu Collaborative Innovation Center of Atmospheric Environment and Equipment Technology (CICAEET), Nanjing University of Information Science & Technology, Jiangsu 210044, China

3. Ministry of Education Key Laboratory for Earth System Modeling, Center for Earth System Science, Tsinghua University, Beijing 100084, China

4. Jiangsu Provincial Academy of Environmental Science, 176 North Jiangdong Rd., Nanjing, Jiangsu 210036, China

*Corresponding author: Yu Zhao

Phone: 86-25-89680650; email: yuzhao@nju.edu.cn

Atmos. Chem. Phys. Discuss., doi:10.5194/acp-2016-567, 2016
Manuscript under review for journal Atmos. Chem. Phys.
Published: 25 July 2016

Atmospheric Chemistry and Physics Discussions

ABSTRACT

Improved emission inventories combining detailed source information are crucial for better understanding the atmospheric chemistry and effectively making emission control policies using air quality simulation, particularly at regional or local scales. With the downscaled inventories directly applied, chemical transport model (CTM) might not be able to well reproduce the evolution of atmospheric pollution process at small spatial scales. Using the bottom-up approach, a high-resolution emission inventory was developed for Jiangsu China, including SO_2, NOx, CO, NH_3, volatile organic compounds (VOCs), total suspended particulates (TSP), PM_{10}, $PM_{2.5}$, black carbon (BC), organic carbon (OC), and CO_2. The key parameters relevant to emission estimation for over 6000 industrial sources were investigated, compiled and revised at plant level based on various data sources and on-site survey. As a result, the emission fractions of point sources were significantly elevated for most species. The improvement of this provincial inventory was evaluated through comparisons with other inventories at larger spatial scales, using satellite observation and air quality modeling. Compared to the downscaled Multi-resolution Emission Inventory for China (MEIC), the spatial distribution of NO_X emissions in our provincial inventory was more consistent with summer tropospheric NO_2 VCDs observed from OMI, particularly for the grids with moderate emission levels, implying the improved emission estimation for small and medium industrial plants by this work. Three inventories (national, regional, and provincial by this work) were applied in the Models-3/Community Multi-scale Air Quality (CMAQ) system for southern Jiangsu, to evaluate the model performances with different emission inputs. The best agreement between available ground observation and simulation was found when the provincial inventory was applied, indicated by the smallest normalized mean bias (NMB) and normalized mean errors (NME) for all the concerned species SO_2, NO_2, O_3 and $PM_{2.5}$. The result thus implied the advantage of improved emission inventory at local scale for high resolution air quality modeling. Under the unfavorable meteorology for pollution transport, in particular, much higher SO_2 concentrations than observation were simulated for downtown Nanjing (the capital city of Jiangsu) using the regional or national inventories, implying the overestimation in urban emissions when the locations of large emitters were not fully

Atmos. Chem. Phys. Discuss., doi:10.5194/acp-2016-567, 2016
Manuscript under review for journal Atmos. Chem. Phys.
Published: 25 July 2016

Atmospheric Chemistry and Physics Discussions

considered, and the densities of economy or population were simply applied to downscale or allocate the emissions. With more accurate spatial distribution of emissions at city level, the simulated concentrations using the provincial inventory were much closer to observation. Sensitivity analysis of $PM_{2.5}$ and O_3 formation was conducted using the improved provincial inventory through the Brute Force method. Iron & steel and cement plants were identified as important contributors to the $PM_{2.5}$ concentrations in Nanjing (the capital city of Jiangsu). The O_3 formation was VOCs-limited in southern Jiangsu, and the concentrations were negatively correlated with NO_X emissions in urban areas owing to the accumulated NOx from transportation. More evaluations are further suggested for the impacts of speciation and temporal and vertical distribution of emissions on air quality modeling at regional or local scales in China.

1 INTRODUCTION

With rapid development of economy and growth of energy consumption, eastern China is experiencing severe atmospheric pollution attributed to the large emissions of primary air pollutants and the subsequent formation of secondary pollution, e.g., fine particles and O_3. Relatively high concentrations of surface $PM_{2.5}$ were observed in eastern China based on the national monitoring network (data source: http://106.37.208.233/), and only 9.5% out of 190 cities with the measurement data reported in 2014 met the National Ambient Air Quality Standard (NAAQS), i.e., 35 $\mu g/m^3$ for annual $PM_{2.5}$ concentration (MEP, 2012). Under the serious air pollution, series of measures have been conducted to reduce the pollutant emissions and to improve the air quality across the country. Issued in 2013, for example, the National Air Pollution Prevention Action Plan required strict emission controls on both industry and transportation sectors, and aimed to achieve a 25%, 20% and 15% reduction of annual $PM_{2.5}$ concentration for Beijing-Tianjin-Hebei (JJJ), Yangtze River Delta (YRD), and Pearl River Delta (PRD) region from 2012 to 2017, respectively. Given the non-linear response of ambient concentrations to emissions, chemical transport modeling (CTM) has been widely applied to study the mechanisms of complex pollution processes and the impacts of emission abatement (Zhang et al., 2006; Streets et al., 2007; B. Zhao et al., 2013; Zhang et

Atmos. Chem. Phys. Discuss., doi:10.5194/acp-2016-567, 2016
Manuscript under review for journal Atmos. Chem. Phys.
Published: 25 July 2016

Atmospheric Chemistry and Physics Discussions

al., 2012). As the key input of CTM, therefore, improved emission inventories, particularly at regional or local scales, become important for scientific air quality simulation and effective policy making.

Progress has been increasingly achieved in emission inventory studies for China. Compared to earlier national emission inventories including those for Transport and Chemical Evolution over the Pacific Mission (TRACE-P, Streets et al., 2003), Intercontinental Chemical Transport Experiment-Phase B (INTEX-B, Zhang et al., 2009), and Regional Emission inventory in Asia (REAS, Ohara et al., 2007; Kurokawa et al., 2013), Tsinghua University developed the Multi-resolution Emission Inventory for China (MEIC, http://www.meicmodel.org/), in which the information of large power plants and cement factories was investigated and the uncertainties of emission estimation for those typical sources were reduced (Wang et al., 2014). Besides, high-resolution emission inventories at regional and city scales were gradually established in the developed regions JJJ, YRD and PRD, attributed to better data support and stronger need to combat air pollution (Zheng et al., 2009; S. Wang et al., 2010; Huang et al., 2011; B. Zhao et al., 2012; Zhao et al., 2015).

Resulting from various methods and data sources, clear discrepancies exist in different emission inventories in China, both at national (Y. Zhao et al., 2013; Xia et al., 2016) and local scales (Zhao et al., 2015). When applied in CTM, the uncertainties in emission estimation would inevitably lead to bias in air quality simulation, besides the errors of meteorological field modeling and deficiencies of built-in atmospheric chemical mechanisms (Zheng et al., 2012). Based on the Models-3/Community Multi-scale Air Quality (CMAQ) system, for example, Zhang et al. (2014) simulated $PM_{2.5}$ and O_3 concentrations in southeastern United States using the different versions of national emission inventory (NEI), and compared the results with several ground observational datasets. The model performance with updated inventory (NEI05) was much better than that with old one (NEI99), indicating the impacts of emission inventory on the accuracy of CMAQ simulations. Han et al. (2015) conducted NO_2 vertical column simulation for China with CMAQ, and found that the modeled results using INTEX-B inventory were closer to satellite observation than those using REAS. At regional or local scales, emission inventory that incorporates the detailed information of individual sources is assumed to have advantages in air quality research prior

Atmos. Chem. Phys. Discuss., doi:10.5194/acp-2016-567, 2016
Manuscript under review for journal Atmos. Chem. Phys.
Published: 25 July 2016

Atmospheric Chemistry and Physics Discussions

to downscaled national inventory that generally applied regional average levels of emission factors due to unavailability of data (Zhao et al., 2015). The benefits of improved emission estimation, spatial and temporal distribution, or chemical speciation of pollutants, however, have not been sufficiently confirmed with CTM. Recently, Yin et al. (2015) conducted CMAQ simulation on O_3 using updated VOC emission inventory for PRD, implying that the reduced uncertainties of total emission level and spatial distribution could improve the model performance compared with ground observation.

We select Jiangsu, a typical province with well-developed industry in eastern China, to develop and evaluate the high-resolution emission inventory. The geographic location and cities of the province are illustrated in Figure S1 in the supplement. With a total area of 107 200 km^2 and population of 79.2 million in 2012, Jiangsu was the first ranked province in gross domestic product (GDP) per capita in China (NBSC, 2013a; JSNBS, 2013). It accounted for 8.0%, 7.6%, 8.9%, and 10.2% of the country's power generation, cement, pig iron, and crude steel production in 2012, respectively (NBSC, 2013b). Intensive energy consumption and industry resulted in heavy air pollution: all the 13 cities had their annual average concentrations of $PM_{2.5}$ exceeding the NAAQS in 2012, with the highest reaching 74 $\mu g/m^3$ in the capital city, Nanjing. Clear uncertainties exist in current multi-scale emission inventories. Zhao et al. (2015), for example, estimated Nanjing's SO_2 and $PM_{2.5}$ emissions at 165 and 71 Gg in 2012, respectively, while the results by Fu et al. (2013) were 131.8 and 35.3 Gg, implying the necessity of improvement and assessment of regional emission inventory, for both scientific and policy implication. In this work, a comprehensive emission inventory for Jiangsu with high temporal and spatial resolutions was first established with the best available data of local emission sources incorporated. This provincial emission inventory was then compared with other inventories and satellite observation to test its improvement on emission estimation and spatial distribution. CMAQ was further applied to indicate the advantage of the provincial inventory prior to downscaled national and regional ones. In particular, the impacts of spatial distribution of emissions on model performance were analyzed for period with unfavorable meteorological condition. Finally, the improved inventory was applied for sensitivity analysis on regional $PM_{2.5}$ and O_3 formation.

Atmos. Chem. Phys. Discuss., doi:10.5194/acp-2016-567, 2016
Manuscript under review for journal Atmos. Chem. Phys.
Published: 25 July 2016

Atmospheric Chemistry and Physics Discussions

2 DATA AND METHODS

2.1 Methodology of provincial emission inventory development

The emissions of gaseous pollutants (SO_2, NOx, CO, NH_3 and VOCs), greenhouse gas CO_2, particulate matter (total suspended particulates (TSP), PM_{10} and $PM_{2.5}$) and its chemical compositions (black carbon, BC and organic carbon, OC) of anthropogenic origin in Jiangsu were estimated with a bottom-up method. Emission sources were classified into seven main categories, including power plants, industry, solvent usage, transportation, residential & commercial, agriculture and others. Industry was subdivided into iron & steel, cement, and other industry including nonferrous metal smelting, brick and lime kilns, chemical industry and other industry boilers. Residential & commercial sector included household combustion of fossil fuel and biofuel. Agriculture included livestock and fertilizer usage. Open biomass burning, cooking, and waste (water) disposal, were considered as other sources. The detailed categories were summarized in Table S1 in the supplement. For each category, point, mobile and area sources were defined depending on the detailed levels of information and the emission characteristics, For point sources, information on emission factor and activity level was investigated and compiled for individual plants, and the annual emissions of atmospheric pollutants were calculated using Eq. (1), as described in Zhao et al (2015) :

$$E_i = \sum_{j,m} AL_{i,j,m} \times EF_{i,j,m} \times (1-\eta_{i,j,m}) \quad (1)$$

where i, j and m represented the pollutant species, individual plant, and fuel/technology type, respectively; AL was the activity level data; EF was the uncontrolled emission factor; and η was removal efficiency of air pollutant control device.

Regarded as mobile sources, the emissions of on-road transportation were calculated by the CORPERT model (EEA, 2012) and then spatially allocated based on the road net information of the province. Area sources include non-road transportation, solvent use, residential & commercial sector, agriculture, and small industry plants without detailed information collected. The emissions from non-road transportation and agriculture were estimated following the methods by Zhang et al. (2010) and Dong et al. (2009), respectively.

2.2 Activity level

Most of coals in Jiangsu were used by power and industry sectors, and household

Atmos. Chem. Phys. Discuss., doi:10.5194/acp-2016-567, 2016
Manuscript under review for journal Atmos. Chem. Phys.
Published: 25 July 2016

Atmospheric Chemistry and Physics Discussions

accounted for only 0.3% of total coal consumption in the province in 2012 (JSNBS, 2013), indicating the significance to reduce the uncertainties of emission estimation for power and industry plants. Therefore a comprehensive database for power and industrial sectors was established with the information collected and modified from the official environmental statistics, Pollution Source Census (PSC, internal data), and on-site survey on large emitters. Parameters including geographical location, combustion/production technology, fuel/burner/boiler type, installed air pollution control device (APCD) and its removal efficiency were investigated for individual plants. Totally 6750 plants were identified as point sources, including 191 power plants, 185 iron & steel plants, 231 cement factories, 707 lime and brick factories, 365 chemical plants and 5071 other industrial factories, as illustrated in Figure S2 in the supplement. In particular, the kilns for combustion and factories for calcination were separately investigated for cement production, and 25% of cement plants contained the both processes. For power, cement, and iron & steel sectors, the aggregated activity levels compiled plant by plant, i.e., the coal consumption of power generation, and the production of cement, clinker, coke, pig iron, and crude steel, were estimated at 108%, 95%, 120%, 109%, 104%, and 98% of the provincial statistics, respectively (JSNBS, 2013). The comparison indicates, on one hand, that larger activity levels would be obtained based on detailed investigation of individual emission sources than official statistics for power and most processes of iron & steel sectors. On the other hand, almost completed investigation on point sources was conducted for those sectors, as very small fractions of activities (5% for cement and 2% for steel production) had to be estimated as area sources. For other industrial sectors, smaller fractions of point sources were obtained, e.g., 32% and 36% for ammonia and sulfuric acid production, respectively.

For on-road transportation, the input parameters of COPERT 4 include regional meteorological information, vehicle population by type, fleet composition by control stage (China I–IV, equivalent to Euro I–IV), average vehicle speeds, and annual average kilometers traveled (VKT). Monthly mean temperature and relative humidity were obtained from the China Meteorological Data Sharing Service System (http://www.escience.gov.cn). Populations of different vehicle types were derived from statistical yearbooks by city and then adjusted in accordance with the model requirement. The fleet composition by control stage

Atmos. Chem. Phys. Discuss., doi:10.5194/acp-2016-567, 2016
Manuscript under review for journal Atmos. Chem. Phys.
Published: 25 July 2016

Atmospheric Chemistry and Physics Discussions

was obtained from the survey by local government (internal data, Zhao et al., 2015). Vehicle speed by road type (i.e., freeway, arterial and residential road) and VKT by vehicle type were determined according to previous studies (Cai and Xie, 2007; Wang et al., 2008) and the guidebook of emission inventory development for Chinese cities (He, 2015). For area sources, the coal consumption of residential & commercial activities was directly taken from National Energy Statistic Yearbook (NBSC, 2013c), while that of small industrial plants were calculated as the coal consumption of total industry from the provincial energy balance (NBSC, 2013c) minus the coal consumption of industrial point sources. The original data on the activity levels of agriculture, solvent use, non-road transportation and open biomass burning were obtained from the provincial or city statistical yearbooks (JSBNS, 2013).

2.3 Emission factor

Following previous studies (Zhao et al., 2008; 2010; 2011; 2012a; 2012b; Y. Zhao et al., 2013), an emission factor database for Jiangsu was established with detailed information and available results of emission measurements on local sources incorporated. For power sector, parameters relevant to emission factors were obtained at individual plant level including installed capacity, fuel type and quality (e.g., sulfur and ash content), combustion technology, and the type and removal efficiencies of APCDs. In particular, the information of APCD installation obtained from provincial environmental statistics and on-site survey was further corrected according to the official documents on APCD projects of power plants published by Ministry of Environment Protection of China (http://www.zhb.gov.cn/gkml/hbb/bgg/201305/t20130506_251654.htm). As summarized in Table S2 in the supplement, the application rates of flue gas desulfurization (FGD), selective catalytic reduction (SCR)/selective non-catalytic reduction (SNCR), and dust collectors for Jiangsu's power plants in 2012 were 97%, 57% and 99% in terms of coal consumption, and the average removal efficiencies of SO_2, NOx and TSP weighted by coal consumption were calculated at 83.3%, 37.1% and 98.0%, respectively. Combining all the above-mentioned information, the emission factors for individual plant and facility were calculated using the methods developed by Zhao et al. (2010).

For iron & steel production, emission factors of the four main manufacturing processes

Atmos. Chem. Phys. Discuss., doi:10.5194/acp-2016-567, 2016
Manuscript under review for journal Atmos. Chem. Phys.
Published: 25 July 2016

(coking, sintering, pig iron production, and steel making) were estimated combining the unabated emission factors from previous database (Zhao et al., 2011; Y. Zhao et al., 2013) and the investigated information on penetrations and removal efficiencies of APCDs at plant level. Provided in Table S2, 64.3% of Jiangsu's iron & steel plants installed FGD in 2012 and the average SO_2 removal efficiency was estimated at 78.0%. Dust collectors were installed at almost all the furnaces for pig iron production and steel making, with the averages of PM removal efficiency estimated at 96% and 94%, respectively. For cement production, emission factors were calculated for the two main processes, coal combustion and calcination, following Lei et al. (2011). With dust collectors installed at 99% of plants, the average of overall removal efficiency on TSP was estimated at 97.3% according to our plant-by-plant investigation (Table S2).

For area sources, emission factors for non-road transportation were obtained from Zhang et al. (2010), Ye et al. (2014) and Fu et al. (2012). Emission factors for household fossil fuel and biofuel combustion were from the summary of field measurements in Y. Zhao et al. (2013). For agricultural activities including livestock and fertilizer use, emission factors were obtained from Dong et al. (2009) and Yin et al. (2010). Emission factors of VOCs were mainly from Wei et al. (2009) with update for typical sources based on limited local measurements and survey (Bo et al., 2008; EEA, 2013; Xia et al., 2014).

2.4 Temporal and spatial distributions

The monthly variations of emissions from power plants and industrial sources were assumed to be dominated by with the variations of electricity generation and typical industrial production, respectively, and those data were obtained from National Bureau of Statistics of China (http://data.stats.gov.cn/). As the real-time monitoring on urban traffic was unavailable for the whole province, the temporal distribution of emissions from on-road vehicles in other cities was considered to the same as Nanjing (Zhao et al., 2015). For other sources, the temporal distributions in Shanghai investigated by Li et al. (2011).

Different parameters were used to conduct the spatial allocation of emissions by sector. Latitude and longitude of each point source collected from PSC were checked and revised according to Google Earth to avoid the unexpected errors in the existing database. The

Atmos. Chem. Phys. Discuss., doi:10.5194/acp-2016-567, 2016
Manuscript under review for journal Atmos. Chem. Phys.
Published: 25 July 2016

densities of GDP and population were applied to allocate the emissions from industrial area sources, and residential and commercial sources, respectively. Emissions from on-road transportation were allocated based on the road net by city. As the ship flow was unavailable, the widths of Yangtze River and the Grand Cannel within Jiangsu were used as indicators for ship emissions. Emissions from open biomass burning were allocated by the locations and brightness of agricultural fire spots observed by MODIS (Moderate Resolution Imaging Spectroradiometer, https://earthdata.nasa.gov/data/near-real-time-data/firms). NH_3 emissions from livestock and fertilizer use were allocated by the density of rural population.

2.5 Configuration of air quality modeling

The Models-3/Community Multi-scale Air Quality (CMAQ) version 4.7.1 was applied to evaluate the emission inventory for Jiangsu. As shown in Figure 1, three one-way nested domain modeling was conducted, and the spatial resolutions were set at 27, 9 and 3 km respectively in Lambert Conformal Conic projection, centered at (110° E, 34° N) with two true latitudes 25°N and 40°N. The mother domain (D1, 180×130 cells) covered most part of China, Japan and the whole Korea and part of other country. Jiangsu, Zhejiang, Shanghai, Anhui and parts of other provinces were at the second modeling region (D2, 118×97 cells). The third (D3, 124×70 cells) covered the mega city Shanghai and six most developed cities in southern Jiangsu including Nanjing, Changzhou, Zhenjiang, Wuxi, Suzhou and Nantong. The simulation period was selected from October 1 to 31, 2012, with the first five days chosen as spin-up period to provide initial conditions for later simulations.

Meteorological fields were provided by the Weather Research and Forecasting Model (WRF) version 3.4 with the main physical options set as Fu et al. (2014), and the outputs were transferred by meteorology chemistry interface professor (MCIP) version 4.2 into the chemistry transport module in CMAQ (CCTM). In WRF, the U.S. Geological Survey (USGS) database was adapted as terrain and land use data, and the first guess field of meteorological modeling was provided by the final analysis dataset (ds083.2) from National Centers for Environmental Prediction (NCEP). Statistical indicators including Bias, Index of Agreement (IOA), and root mean squared error (RMSE) were applied to evaluate the performance of WRF modeling against observation (Baker, 2004; Zhang et al., 2006). Ground observations in

Atmos. Chem. Phys. Discuss., doi:10.5194/acp-2016-567, 2016
Manuscript under review for journal Atmos. Chem. Phys.
Published: 25 July 2016

Atmospheric Chemistry and Physics Discussions

three hours interval at meteorological stations were downloaded from National Climatic Data Center (NCDC), including 43 stations in the second modeling domain D2 and 7 stations in the innermost domain D3 (as labeled in Figure 1). The statistics of those indicators for wind speed and direction at 10 m (WS10 and WD10), temperature at 2 m (T2) and relative humidity at 2 m (RH2) for October 2012 in D2 and D3 were summarized in Table S3. Discrepancies between WRF simulations and ground observations were within acceptable range (Emory et al., 2001) and comparable to the results of other studies (Wang et al., 2014). Better agreements were found for simulations of T2 and RH2 than WS10 and WD10. In spite of moderate overestimation by 0.3% and 3.5% in T2 and RH2, the IOA of those two variables were 0.97 and 0.90, indicating the high consistency with observationa. Slightly higher than observation in D2 and D3, simulated WS10 might enhance the diffusion process of pollutants in atmosphere eventually and thus lead to underestimation in pollutant concentrations. For WD10, the bias between simulations and observations was 3.6 degree in D3 within the benchmark range (Emory et al., 2001).

The carbon bond gas-phase mechanism (CB05) and AERO5 aerosol module were adopted in all the CMAQ modules. The initial and boundary conditions for first modeling domain was the default clean profile, while for nested domain they were extracted from the CCTM outputs of its mother domain. Anthropogenic emissions used for domains D1 and D2 were obtained from the downscaled MEIC with an original spatial resolution of 0.25°×0.25°. For Jiangsu domain in D3, three inventories, i.e., downscaled MEIC, the regional inventory of YRD by Fu et al. (2013), and the provincial inventory developed in this work, were used to test the modeling performance and potential improvement in emission estimation. In addition, biogenic emission inventory were from the Model Emissions of Gases and Aerosols from Nature developed under the Monitoring Atmospheric Composition and Climate project (MEGAN-MACC, Sindelarova et al., 2014), and the emission inventories of Cl, HCl and lightning NO_X were from the Global Emissions Initiative (GEIA, Price et al., 1997). The vertical distribution of emissions was determined by source following L. Wang et al. (2010).

Atmos. Chem. Phys. Discuss., doi:10.5194/acp-2016-567, 2016
Manuscript under review for journal Atmos. Chem. Phys.
Published: 25 July 2016

Atmospheric Chemistry and Physics Discussions

3 RESULTS

3.1 Emission estimation and sector contribution

The total annual emissions of SO_2, NOx, CO, TSP, PM_{10}, $PM_{2.5}$, BC, OC, CO_2, NH_3 and VOCs were calculated at 1142, 1642, 7680, 2606, 1394, 941, 57, 138, 860458, 1100 and 1747 Gg for Jiangsu in 2012, respectively. The emissions by city were provided in Table 1. In general, higher emissions were found in cities in southern Jiangsu with large population and intensive economy and industry than those in northern Jiangsu. Taking 52% of the provincial industrial GDP, Suzhou, Nanjing, and Wuxi were estimated to collectively account for 41%, 41%, 35%, 31%, 43% and 39% of the total emissions of SO_2, NOx, CO, $PM_{2.5}$, CO_2 and VOCs, respectively. Xuzhou, different from other cities in northern Jiangsu, had a relative high emissions of pollutants due to its well development of large-scale industry. Because of the active agricultural development, NH_3 emissions in Huai'an and Nantong were estimated at 195.9 and 187.1 Gg, significantly higher than other cities.

Shown in Figure 2 is the detailed sector contribution of pollutants from point, mobile (on-road transportation) and area sources. The point sources including power and industrial plants contributed 84%, 71%, 55%, 83%, 75%, 64%, 41%, 31%, 83%, 2% and 36%, to the total emissions of SO_2, NOx, CO, TSP, PM_{10}, $PM_{2.5}$, BC, OC, CO_2, NH_3 and VOCs, respectively. The emission fractions of point sources were notably larger than those in other regional inventories (Fu, 2009; Tang et al., 2012; B. Zhao et al., 2012), resulting mainly from the compiling and application of information on individual power and industrial plants from varied data sources. Defined as area source, open biomass burning contributed 12%, 19%, 23%, 11% and 41% to the total CO, PM_{10}, $PM_{2.5}$, BC and OC, respectively.

The dominant contributors to SO_2 were power plant, iron & steel and other industry, with the emission fractions estimated at 38%, 10% and 45%, respectively. Although the coal consumption in power sector was 3.5 times larger than that in other industry sector (cement and iron & steel production excluded, JSNBS, 2013), smaller contribution to SO_2 emissions were found for coal-fired power plants, implying the benefits of strict control on SO_2 emissions from power sector. As shown in Table S2, the application rate and average SO_2 removal efficiency of FGD in power sector were significantly higher than those in other

Atmos. Chem. Phys. Discuss., doi:10.5194/acp-2016-567, 2016
Manuscript under review for journal Atmos. Chem. Phys.
Published: 25 July 2016

Atmospheric Chemistry and Physics Discussions

industry, suggesting the improvement in SO_2 abatement for industrial coal combustion other than power plants would be an effective measure to further reduce the emissions.

Power sector was the largest source for NO_X, contributing 41% to the total emissions, while the share of coal consumption of the sector reached 65% (JSNBS, 2013). It thus implied the tightened controls from implementation of new emission standard (GB13223-2011) and improved use of SCR/SNCR on power plants since 2011 compared to other sectors. Compiled from unit level, the average NOx removal efficiency of SCR/SNCR was calculated at 37% for Jiangsu's power plants in 2012 (Table S2), while Tian et al. (2013) estimated the values for SCR and SNCR at 70% and 25%, respectively, indicating the differences in assessment of emission controls for power sector between the provincial and national emission inventories with varied data sources. Transportation (including on-road and non-road) was estimated to be the second largest sector for NO_X emissions, with the share to the total emissions calculated at 24%. Without specific control measures, cement and other industry were estimated to account for 7% and 17% of total NOx emissions.

CO was mainly generated from the manufacturing processes in iron & steel plants. The production of pig iron and crude steel in Jiangsu accounted for 9% and 10% to the national total in 2012, respectively (NBS, 2013), and was higher than other provinces in China except Hebei. Due to the intensive iron & steel industry, the contribution of the sector to the provincial total CO emissions was estimated at 35%. Residential biofuel combustion, open biomass burning and on-road transportation were also large contributors to CO with the emission fractions calculated as 24%, 12% and 11% respectively.

For particles, iron & steel and cement production were estimated to be the largest sources, contributing 24% and 27% to the total emissions of PM_{10}, and 27% and 19% to $PM_{2.5}$, respectively. Even with the largest coal consumption among all the sectors, the emissions from power plants were relatively small (6% and 4% to PM_{10} and $PM_{2.5}$ emissions, respectively), resulting mainly from the relatively high penetrations and removal efficiencies of dust collectors. Great differences existed in the sector distribution of BC and OC emissions. Iron & steel was estimated to be the largest source of BC, while open biomass burning and biofuel burning in residential stoves dominated OC, with the shares estimated at 41% and 29%, respectively. Moreover, as BC exhausted from the diesel engines was demonstrated to

Atmos. Chem. Phys. Discuss., doi:10.5194/acp-2016-567, 2016
Manuscript under review for journal Atmos. Chem. Phys.
Published: 25 July 2016

be higher than OC in previous situ measurements (He et al., 2015), BC emissions from non-road transportation (agricultural machines, rural vehicles, ships and construction machines) was estimated more than twice larger than OC.

For VOCs, solvent use and other industry including oil refinery, chemical industry and combustion were identified as the largest sources contributing 30% and 29% to total emissions, respectively. In particular, oil refinery and chemical engineering collectively accounted for 74% of the emissions of other industry. Due to lack of investigation on chemical industry plants, the fraction of area sources to the emissions of other industry reached 35%. Transportation and residential cooking are estimated to contribute 12% and 4% to total VOCs emissions, respectively. Livestock and fertilizer use were the two dominating sources of NH_3, with the shares to total emissions estimated at 47% and 45%, respectively. For industry, ammonia production was the main source accounting for half of NH_3 emissions.

The spatial distribution of SO_2, NOx, CO, $PM_{2.5}$, VOCs and NH_3 emissions at a resolution of 3×3km were illustrated in Figure S3 in the supplement. Outstandingly high emissions of SO_2, NOx, $PM_{2.5}$ and VOC indicated the existence of large industrial plants, particularly in Suzhou, Nanjing and Wuxi along with the Yangtze River. For CO and NOx, large emissions were distributed along the road net in the province, reflecting the important contribution of on-road transportation. Unlike other pollutants, high NH_3 emissions were more evenly distributed in rural areas as dominated by agricultural activities.

3.2 Comparisons with other studies

Figure 3 compares the emission estimations for Jiangsu between our provincial inventory and previous studies including two regional inventories (Fu et al., 2013; Li et al., 2011) and two national ones (MEIC; Xia et al., 2016). Note this work and Xia et al. (2016) reported the numbers for 2012, while Fu et al. (2013), Li et al. (2011) and MEIC for 2010. As the emissions from open biomass burning were not included in other inventories except Fu et al. (2013) and this work, two values labeled as A and B were provided for our provincial inventory indicating the emissions without and with biomass open burning, respectively. While provincial economy and energy data were generally applied in all the national/regional inventories, information of individual large emitters were incorporated as well in MEIC, Fu et

Atmos. Chem. Phys. Discuss., doi:10.5194/acp-2016-567, 2016
Manuscript under review for journal Atmos. Chem. Phys.
Published: 25 July 2016

Atmospheric Chemistry and Physics Discussions

al. (2013) and Li et al. (2011). For example, the emissions of big plants for power generation, iron & steel and cement production in Jiangsu were partially investigated in Fu et al. (2013) and Li et al. (2011). For MEIC, large fraction of emissions from power generation sector was calculated plant by plant with relatively good data availability, while emissions from other industrial sectors were basically calculated at regional average and spatially allocated as area sources. The results in Fu et al. (2013) were generally smaller than those in other two inventories for 2010.

Attributed mainly to the improved use of FGD, the total SO_2 emissions were estimated to decline from 2010 to 2012 for the whole country (Xia et al., 2016) and typical city in Jiangsu (Zhao et al., 2015). It was reasonable to some extent that the SO_2 emissions in Jiangsu estimated in this work for 2012 was less than the 2010 results by Li et al. (2011) and MEIC. Our estimation was 15% lower than the result for Jiangsu extracted from the national inventory by Xia et al. (2016), due mainly to the discrepancies in the penetration and SO_2 removal efficiency of FGD applied in the two inventories. Such information was obtained at provincial or national average level by Xia et al. (2016), in contrast to the provincial inventory based on investigation at plant level. For example, Xia et al. (2016) assumed that the penetration rates of wet and dry FGD technologies in coal-fired power sector were 83% and 5% in 2012, with the removal efficiencies estimated at 80% and 40%, respectively, and that there was not any SO_2 control in the remaining 11% of installed capacity at all. According to our plant-based investigation, the controls in Jiangsu were clearly enhanced, as shown in Table S2. As a result, SO_2 emissions from power sector was calculated at 430.0 Gg for Jiangsu 2012 in this work, 42% lower than those in Xia et al. (2016). The result for 2012 in our provincial inventory, however, is very close to the estimation by MEIC for 2010 (437.4 Gg), even though the coal consumption of power generation increased 29% for the period 2010-2012 (JSNBS, 2013). Besides the uncertainty in emission estimation from varied data sources of the two inventories, the improved use of FGD in the sector could be an important reason for the restrained emissions. Similar fact was found for Nanjing, the capital city of Jiangsu, that the SO_2 emissions of power generation calculated at city level kept stable along with a 25% growth of coal consumption from 2010 to 2012 (Zhao et al., 2015).

NOx emissions in our provincial inventory was slightly higher than those of Li et al.

Atmos. Chem. Phys. Discuss., doi:10.5194/acp-2016-567, 2016
Manuscript under review for journal Atmos. Chem. Phys.
Published: 25 July 2016

Atmospheric Chemistry and Physics Discussions

(2011) and clearly lower than the two national inventories. The major difference between the provincial inventory and MEIC was from industry, attributed probably to the application of varied emission factors. With different methods and data sources for certain sectors, the NOx emissions from industry were calculated at 388.1 and 566.2 Gg respectively by this work and Xia et al. (2016). For on-road transportation, the emission factors were estimated using CORPERT in this work, while they were obtained from limited domestic measurements in Xia et al. (2016). That was also the most important reason for the discrepancies in CO emission estimation between the two studies. For 2010, the NO_X emissions estimated by Fu et al. (2013) was 18% and 36% lower than those by Li et al. (2011) and MEIC, resulting mainly from the higher application rate and removal efficiency of SCR/SNCR technologies for power sector used in Fu et al. (2013).

The $PM_{2.5}$ and PM_{10} emissions in the provincial inventory were estimated to be 6% and 23% higher than those of Xia et al. (2016), and the sector contributions were notably different in the two inventories. For example, industry was estimated to contribute 77% and 80% of $PM_{2.5}$ and PM_{10} in the provincial inventory, much larger than the fractions at 45% and 52% by Xia et al. (2016), respectively. In this work, the $PM_{2.5}$ and PM_{10} emissions from cement production were calculated at 181 and 384 Gg, i.e., 2.5 and 2.0 times to those in Xia et al. (2016), and the analogue numbers for iron & steel production were 134 and 263 Gg, and 1.8 and 1.7 times, respectively. The discrepancies resulted mainly from the inconsistent penetration rates and removal efficiencies of dust collectors determined at national level and from on-site survey at provincial level. Taking cement as an example, all the plants were assumed to be installed with dust collectors, and the national average removal efficiency at 99.3% was applied in Xia et al. (2016), clearly larger than that from plant-by-plant survey as shown in Table S2. Note that the particle emissions in the provincial inventory were estimated higher than those in national ones including MEIC and Xia et al. (2016), while the gaseous pollutant emissions were lower except for NH_3 and CO_2. It thus implied that the control of SO_2 and NOx in Jiangsu were stronger than the national average level but weaker for particles. Compared to the emissions for 2010 estimated by other studies, the $PM_{2.5}$ and PM_{10} in our provincial inventory were 58% and 56% larger than Fu et al. (2013) (biomass open burning included), and 24% and 25% larger than Li et al. (2011) (biomass open burning excluded),

Atmos. Chem. Phys. Discuss., doi:10.5194/acp-2016-567, 2016
Manuscript under review for journal Atmos. Chem. Phys.
Published: 25 July 2016

Atmospheric Chemistry and Physics Discussions

441 respectively, beyond the growth rate of 20% for coal consumption during 2010-2012 (NBS,
442 2011; 2013).

443 The NH_3 emissions of Fu et al. (2013) and Li et al. (2011) were close to each other, while
444 MEIC was only half of them for 2010. Using the results for 2006 from Huang et al. (2012),
445 MEIC made a very low estimation in NH_3 emissions from livestock. The NH_3 emissions for
446 2012 in this work was calculated 11% and 22% larger than the results for 2010 by Fu et al.
447 (2013) and Li et al. (2011), respectively. The agricultural GDP increased 35% from 2010 to
448 2012 in Jiangsu (JSNBS, 2013), thus the growth of activity levels were expected to result in
449 enhanced emissions, as very little progress was achieved for NH_3 control for these years.

450 **3.3 Analysis of spatial distribution of emissions from given sectors**

451 To further explore the discrepancies in emission estimation and spatial distribution from
452 varied data and emission allocation methods, comparisons between MEIC and our provincial
453 inventory were conducted for pollutants from typical sources, including SO_2 from power
454 plants, NO_X from transportation, and $PM_{2.5}$ from industry. The estimates in this work were
455 reallocated into the 0.25°×0.25° grids, consistent with the spatial resolution of MEIC, and the
456 correlation coefficients for emissions in all the grids can be calculated, as shown in Figure 4.
457 Due mainly to the relatively transparent and easily available information of power plants,
458 good consistency was found for SO_2 emissions from power sector in the two inventories, with
459 the correlation coefficient calculated at 0.7 (Figure 4a). Even though the fundamental
460 information of power plants in China is more accessible than other industry sources,
461 mismatches still exist in different data sources. For example, some emission hotspots in our
462 provincial inventory were not totally identical with those in MEIC in Suzhou, Nantong and
463 Nanjing. In contrast to plant-by-plant investigation, the data from existing statistics at national
464 level could not fully track the actual changes in the emitters, e.g., operation of new-built units,
465 shutting down the small ones, or relocation of individual plants. In MEIC, moreover, the SO_2
466 emissions in several grids were estimated extremely small (less than 1 Mg), indicating that
467 part of emissions from power sector was still allocated as area sources based on density of
468 GDP or population. In contrast, all the plants were identified as point sources in the provincial
469 inventory, based on the thorough investigation on individual sources.

Atmos. Chem. Phys. Discuss., doi:10.5194/acp-2016-567, 2016
Manuscript under review for journal Atmos. Chem. Phys.
Published: 25 July 2016

Atmospheric Chemistry and Physics Discussions

For NO_X from transportation, the correlation coefficient was calculated at 0.8, indicating an even better consistency than SO_2 from power plants between the two inventories (Figure 4b). Although the difference in total emissions was small between our provincial inventory (682 Gg) and MEIC (722 Gg), the estimation of MEIC was notably higher than our result for northern Jiangsu including Yancheng, Huai'an and Suqian, implying the impacts from different ways for emission allocation. In this work, emissions from on-road vehicles were calculated and allocated based on road net that incorporates the information of transportation flow by road grade for each city. For non-road sources, large fraction of emissions was allocated based on the GDP density incorporated with land-use type. In national emission inventories, however, the emissions were first calculated at provincial level, and then downscaled at certain horizontal resolution. Despite of the discrepancies, it could be indicated by the relatively high spatial correlation between the two inventories that using GDP as proxy for emission allocation would be acceptable when detailed information on road net and transportation flow was unavailable, since vehicles were largely concentrated in downtown with the intensive economic activity.

For $PM_{2.5}$ from industry, the correlation coefficient was calculated at 0.335, significantly lower than those mentioned above, indicating larger discrepancy in spatial distribution of industrial emissions between provincial and national inventories compared to power and transportation sectors. As shown in Figure 4c, the emission hotspots in the provincial inventory are highly consistent with the locations of large industrial $PM_{2.5}$ emitters (more than 10 Gg) estimated in this work, while the emission in MEIC were more distributed in developed cities (e.g., Suzhou) with high density of population or economy. Along with fast urbanization, super industrial sources have gradually been relocated to the rural or suburban areas, and the spatial correlation between industrial emissions and population could thus be weakened. In our provincial inventory, most industrial enterprises were identified as point sources, with the key parameters including geographic location, activity level and removal efficiency of dust collector investigated and corrected at plant level. In MEIC, the emissions were calculated using parameters at regional average level and allocated as area sources according to densities of population and/or economic activity. Without detailed information for individual sources, it might lead to errors in emission estimation and spatial distribution at

Atmos. Chem. Phys. Discuss., doi:10.5194/acp-2016-567, 2016
Manuscript under review for journal Atmos. Chem. Phys.
Published: 25 July 2016

regional or local scale. According to the survey at plant level, for example, only 20% of the lime factories were installed dust collectors in Jiangsu 2012, much lower than the value (roughly 90%) assumed in national inventories. As a result, the $PM_{2.5}$ emissions from industry were calculated at 570 Gg in our provincial inventory, 78% higher than those of MEIC.

4 ASSESSMENT OF THE PROVINCIAL EMISSION INVENTORY

4.1 Evaluation of spatial distribution of NO_X emissions with satellite observation

Troposphere NO_2 vertical column density (VCD) retrieved from Ozone Monitoring Instrument (OMI) by the Royal Netherlands Meteorological Institute (Boersma et al., 2011) was employed to test the spatial distribution of NOx emissions in MEIC and this work. NO_2 VCDs in summer were used due to the short lifetime of NO_2 in atmosphere at high temperature and the difficulty in accumulation for primary emissions with strong air convection. In addition, the summer prevailing wind for Jiangsu was generally from southeast where Shanghai and Zhejiang Province are located (see Figure S1 for the locations of the three regions). Total NO_X emissions of Jiangsu were estimated to be 65% and 282% larger than those of Shanghai and Zhejiang Shanghai in MEIC, and local sources were expected to dominate the pollution for the province (Cheng et al., 2011). As Mijling et al. (2013) illustrated satellite observations could be used to evaluate the primary emissions for regions where NO_2 VCDs were mainly affected by local emissions, it was thus feasible to apply the OMI NO_2 VCDs in Jiangsu to assess its NOx emissions.

NO_2 VCDs in July 2010 and 2012 with original spatial resolution of 0.125°×0.125° were used for comparisons with the emissions in MEIC and our provincial inventory, respectively. To be consistent with MEIC, the emissions in our provincial inventory and the NO_2 VCDs from OMI were first upscaled to 0.25°×0.25° for the purpose of visualization and correlation analysis. As can be seen in Figure 5a and 5b, clear reduction in summer NO_2 VCDs was found in southern Jiangsu from 2010 to 2012, indicating the benefits of efforts on NO_X abatement since 2011. The NO_2 VCDs in the area along the Yangtze River were notably higher than that in other regions, attributed possibly to the substantial emissions from vessels and small captive power plants of the chemical and refinery industrial parks along the river

Atmos. Chem. Phys. Discuss., doi:10.5194/acp-2016-567, 2016
Manuscript under review for journal Atmos. Chem. Phys.
Published: 25 July 2016

Atmospheric Chemistry and Physics Discussions

529 without stringent controls as big power plants. Shown in Figure 5c and 5d are the spatial
530 distributions of Jiangsu's NO_X emissions in MEIC and our provincial inventory, respectively，
531 and the emission hotspots were generally consistent between the two inventories. Figure 5e
532 and 5f shows the linear regression results between NO_2 VCDs and NOx emissions in MEIC
533 and the provincial inventory, respectively. The correlation coefficients between VCDs and
534 emissions were separately provided for all the grids and grids in different emission intervals,
535 i.e., top 50%, 50%-75%, and last 25%.

536 The correlation coefficient between NO_2 VCDs and NOx emissions from the provincial
537 inventory was 0.534, close to that between NO_2 VCDs and MEIC at 0.531. The result
538 indicated that there was no significant difference in spatial distribution of emissions between
539 the national and provincial inventories at the relatively low horizontal resolution. However,
540 great discrepancies existed when the correlation analysis was conducted for grids in different
541 emission intervals. As shown in Figure 5e, the correlation coefficients between VCDs and
542 MEIC emissions were calculated at 0.24 and 0.34, respectively, for the top 50% (20 grids with
543 emissions ranged 32-121 Gg) and last 25% of gridded emissions (161 grids with emissions
544 ranged 0-12 Gg) . For our provincial emission inventory, the correlation coefficients were
545 estimated slightly higher at 0.28 and 0.38, respectively, for the top 50% (18 grids with
546 emissions ranged from 30-75 Gg) and last 25% of gridded emissions (176 grids with
547 emissions ranged 0-12 Gg). Moreover, the coefficient between NO_2 VCDs and gridded
548 emissions for the 50% -75% interval in provincial inventory was 0.26, while negative value
549 (-0.07) was calculated for MEIC, indicating that the emission estimation for areas with small
550 and medium plants in the provincial inventory was more consistent with satellite observation.
551 To better quantify the emissions at local scale, the results revealed the practical significance of
552 careful investigation on individual small industrial plants that were usually identified as area
553 sources due to lack of detailed information in national or regional inventories.

554 **4.2 Evaluation of multi-scale inventories with CMAQ**

555 As mentioned in Section 2.5, anthropogenic emission inventories at provincial, regional
556 and national scales were applied respectively to explore the impacts of emission input on the
557 performance of city-scale air quality simulation using CMAQ. With the original horizontal

Atmos. Chem. Phys. Discuss., doi:10.5194/acp-2016-567, 2016
Manuscript under review for journal Atmos. Chem. Phys.
Published: 25 July 2016

Atmospheric Chemistry and Physics Discussions

558 resolutions at 0.25°×0.25° and 4×4 km, respectively, national (MEIC) and YRD regional
559 inventories (Fu et al., 2013) were reallocated into the D3 of CCTM modeling at 3×3 km
560 (Figure 1), consistent with our provincial inventory. The vertical and temporal distributions of
561 the two inventories were assumed to be same as those of our provincial inventory, as indicated
562 in Section 2.4. Given the very limited data accessible on air quality for the province in 2012,
563 the available observation data at nine state-operated monitoring sites in Nanjing including six
564 urban sites (Xuanwumen (XWM), Shanxilu (SXL), Zhonghuamen (ZHM), Ruijinlu (RJL),
565 Caochangmen (CCM), and Maigaoqiao (MGQ)) and three suburban sites (Pukou (PKS),
566 Xianlin (XLS) and Olympic sports center (OSC)) were applied to evaluate the simulation
567 performances with different emission inputs (see locations of the nine sites in Figure 1).

568 The hourly ground concentrations from observation and CMAQ simulation for October
569 2012, expressed as the averages for all the monitoring sites in Nanjing, were compared and
570 illustrated in Figure S4 in the supplement for SO_2, NO_2, O_3 and $PM_{2.5}$. Even though all the
571 simulations could well reproduce the time variation of each species, discrepancies existed
572 when different anthropogenic emission inventories were used. The simulated SO_2 and NO_2
573 concentrations using the provincial inventory were notably lower than those with other two
574 inventories. In addition, simulations could hardly catch the high $PM_{2.5}$ and O_3 concentrations
575 in heavy polluted episode. For example, the average $PM_{2.5}$ ground concentration during
576 October 21st-23rd and 28th-29th were simulated at 40 and 31 μg/m^3, 1.4 and 3.2 times lower
577 than observations. Two statistical indicators, normalized mean bias (NMB) and normalized
578 mean error (NME), were applied to evaluate the model performance (Zhang et al., 2006), as
579 summarized in Table 2. Among all the species, the best simulation performance was found for
580 NO_2, with the NMBs ranged within ±30% for different emission. In general, simulations
581 using the provincial emission inventory performed notably better than those with national and
582 regional ones for all the species, and the NMEs and NMBs were calculated at 47%, 33%,
583 44%%, 52% and -10%, -14%, -25%, -43% for SO_2, NO_2, O_3, $PM_{2.5}$ respectively, comparable
584 to previous U.S. studies (Zhang et al., 2006; Wang et al., 2009). The result thus partly
585 confirmed that air quality simulation at local or regional scale would be largely improved
586 when detailed information on individual sources could be incorporated in the emission
587 inventory. Compared to primary pollutants SO_2 and NO_2, however, species with strong

Atmos. Chem. Phys. Discuss., doi:10.5194/acp-2016-567, 2016
Manuscript under review for journal Atmos. Chem. Phys.
Published: 25 July 2016

Atmospheric Chemistry and Physics Discussions

588 secondary formation process ($PM_{2.5}$ and O_3 in this case) were clearly under predicted by
589 CMAQ, no matter which inventory was applied. Lack of dust emissions in inventories might
590 be one reason for underestimation of $PM_{2.5}$. Moreover, as the significant composition of $PM_{2.5}$
591 in eastern China (Yang et al., 2011), secondary organic and inorganic aerosols might be under
592 predicted attribute to the weakness of chemical mechanisms in the version of CMAQ
593 including the transformation of sulfate and the formation of secondary organic aerosols (Wang
594 et al., 2009). For O_3 simulation, better performance was found at suburban sites than urban
595 sites, and the lower simulated concentrations than observation could possibly come from the
596 underestimation in precursor VOCs emissions. For example, the NMB was estimated at -26%
597 for PKS, where many chemical industrial plants were located nearby. In addition, the
598 uncertainty of NO_X emission estimation might also contribute to the discrepancy. As indicated
599 by the data from available continuous emission monitoring systems on Jiangsu's power plants,
600 the NO_X emission factors of power sector applied in current inventory might be overestimated
601 for 2012 (unpublished).

602 The total emissions of SO_2 and NOx in Jiangsu estimated by Fu et al. (2013) was 1126
603 and 1257 Gg, i.e., 9% and 22% lower than the results of our provincial inventory, respectively.
604 Using the regional inventory by Fu et al. (2013), much higher concentrations of SO_2 and NO_2
605 were simulated than observation at the monitoring sites, with the NMBs calculated at 74%
606 and 30%, respectively. Even with larger emissions, in contrast, the NMBs for simulation with
607 our provincial inventory were -10% and -14%, indicating lower simulated concentrations than
608 observation. This result implies the possible impacts of spatial distributions of emissions on
609 air quality modeling. In regional inventory, densities of population and economic activities
610 were generally applied to allocate large fraction of emissions, leading to particularly high
611 emissions in urban areas, as the economy and population was generally centralized in
612 downtown. Given all the monitoring sites in Nanjing are located in urban or suburban areas,
613 air quality simulation using regional emission inventory was thus liable to over predict the
614 ground concentrations at those sites.

615 Spatial distributions of the monthly mean for simulated concentrations using national,
616 regional and provincial inventories were plotted for SO_2, NO_2, $PM_{2.5}$ and O_3 in Figure 6, and
617 the differences between simulations with varied emissions were shown in Figure 7. As the

Atmos. Chem. Phys. Discuss., doi:10.5194/acp-2016-567, 2016
Manuscript under review for journal Atmos. Chem. Phys.
Published: 25 July 2016

618 MEIC emissions were greatly averaged when they were directly downscaled from
619 0.25°×0.25° to 3×3 km, the simulated high concentrations using MEIC were broadly
620 distributed in the modeling domain and commonly located in downtown (as indicated in
621 Figure S1), with the large emitters hardly identified (Figure 6a). For results using the regional
622 and provincial inventories, there were several grids with notably outstanding simulated
623 concentrations indicating the existence of large emitters (Figure 6b and 6c), and differences
624 with the simulation using MEIC were induced (Figure 7a and 7b). As shown in Figure 7c,
625 moreover, clear differences were also detected between simulations using regional and
626 provincial inventories, implying the discrepancy in allocations of high emissions between the
627 two inventories. With the locations of large power, iron & steel, and cement plants
628 incorporated, the YRD regional emission inventory by Fu et al. (2013) allocated a large
629 fraction of emissions from industries as area sources. In contrast, the emissions from most
630 power and industrial plants were calculated based on source-specific information and were
631 precisely allocated in the provincial inventory, avoiding particularly the emission
632 overestimation in downtown. In addition, the simulated NO_2 and O_3 concentrations for
633 regions outside Jiangsu (i.e., Shanghai and part of Zhejiang and Anhui) using the provincial
634 inventory were 22% lower and 40% higher in average than those using the regional one,
635 respectively (Figure 7c), although same emissions (Fu et al., 2013) were used outside Jiangsu
636 for the two inventories. The result indicated that both local and regional emissions were
637 important for the simulations of the secondary pollutant like O_3. Total VOCs emissions for
638 Jiangsu were estimated at 1740 Gg in MEIC, slight higher than those in the regional (1659 Gg)
639 and provincial inventory (1617 Gg), while the simulated monthly mean O_3 concentrations
640 within Jiangsu using MEIC were notably lower than those using the latter two emissions.
641 Categorized by CB05, differences in chemical compositions of VOCs could be found in the
642 three inventories. For example, the emissions of ethene (ETH) and ethanol (ETHA) with
643 relatively high ozone formation potential in the provincial inventory were 44% and 209%
644 higher than those in MEIC, respectively. Therefore, the total emission amount, spatial
645 distribution of emissions, and the chemical compositions of precursors are all crucial to the
646 accuracy of ozone simulations, and further analysis on those factors are suggested.

Atmos. Chem. Phys. Discuss., doi:10.5194/acp-2016-567, 2016
Manuscript under review for journal Atmos. Chem. Phys.
Published: 25 July 2016

Atmospheric Chemistry and Physics Discussions

4.3 Improved SO_2 simulation under special meteorological condition

To further examine the simulated concentration response to varied emission inputs at local scale, the simulated SO_2 concentrations using national, regional and provincial inventories were compared with observation at three monitoring sites in downtown Nanjing (XWH, RJL and ZHM) for 6th -14th October 2012, as illustrated in Figure 8. The simulated concentrations using our provincial inventory were the most consistent with observation, while apparent overestimation was found for the simulations using national or regional inventories. At 8 pm October 9 (local time), in particular, the SO_2 concentrations were observed at 33, 12, and 14 μg/m^3 at XWH, RJL and ZHM sites, respectively, while the simulated concentrations were respectively simulated at 205, 246 and 228 μg/m^3 using MEIC, i.e., 5-19 times higher than the observation. The analogue numbers with regional inventory by Fu et al. (2013) even reached 550, 477 and 476μg/m^3, i.e., 15-38 times higher than observation. Although concentrations remained over predicted, better performance was achieved when the improved provincial inventory was used, implying its advantage prior to national or regional ones in the high-resolution air quality modeling. The discrepancies in emissions and the simulated meteorological condition including wind velocity and height of planetary boundary layer (PBL) were inspected to understand the very high concentrations from simulation.

Figure S5 in the supplement shows the simulated wind fileds from 2 pm on 9th to 5am on 10th October. From 2 pm on 9th October 9, WS10 in downtown Nanjing started to decline gradually and reached the minimum of 0.22 m/s at 8 pm , simply not beneficial for the horizontal convection of atmosphere. In addition, the monthly average of PBL height at XWH was simulated at 485 m at day and 140 m at night in October. From 5pm on 9th to 10am on 10th, however, the average PBL height decreased to 39m, with the minimum simulated at 32 m at 11pm on 9th , seriously restricting the vertical diffusion of pollutants. Under the meteorological condition that horizontal and vertical movement of atmosphere were limited, primary pollutants from large emitters would be easily accumulated over time, possibly leading to high concentrations for areas close to the emission sources. In this case, therefore, the simulated SO_2 concentrations would be largely influenced by the emissions from local and nearby sources, as discussed below.

Atmos. Chem. Phys. Discuss., doi:10.5194/acp-2016-567, 2016
Manuscript under review for journal Atmos. Chem. Phys.
Published: 25 July 2016

Atmospheric Chemistry and Physics Discussions

677 The total SO_2 emissions in Nanjing were estimated at 141 Gg in the provincial inventory,
678 2% and 7% higher than those of national and regional ones respectively. Without big
679 difference in total amount, large discrepancies in spatial distribution existed in those
680 inventories, particularly at high horizontal resolution as shown in Figure 9. Downscaled from
681 0.25°×0.25° to 3×3 km, grids with similar emissions were clustered for MEIC and spatial
682 variations in emissions could hardly be detected other than the hotspot in downtown (Figure
683 9c). Notably lower emissions in downtown Nanjing were found in our provincial inventory
684 than the regional one (Figure 9a and 9b). In addition, the grid with maximum SO_2 emissions
685 (15.7 Gg) in the provincial inventory was in the northwestern of Nanjing where a super power
686 plant was located, labeled as the black star (point A) in Figure 9. As a comparison, the grid
687 with the maximum SO_2 emissions in the regional inventory labeled as the black triangle (point
688 B) in Figure 9 was adjacent to the location of A, and its emissions were calculated to be only
689 28% of the result in the provincial one. Given no other super emitters located nearby, we
690 expected that the discrepancy resulted mainly from the varied emission estimation and
691 positioning for the same power plant in the two inventories. According to on-site survey, only
692 one unit out of two for the plant was installed with FGD, and the SO_2 emissions of the plant
693 was estimated at 13.6 Gg, accounting for 87% of the total emissions in the grid. In contrast, a
694 higher FGD installation rate at 85% was uniformly assumed for the power sector in the
695 regional inventory by Fu et al. (2013), leading to possible underestimation in emissions for
696 the plant. The comparison implied that detailed information compiled from individual plants
697 was crucial for estimation and spatial distribution of pollutant emissions at local scales. SO_2
698 emissions at given monitoring sites were extracted from the gridded national, regional and
699 provincial inventories and summarized in Table 3. As most large SO_2 emitters were located in
700 suburban or rural areas, relatively small emissions were found in the provincial inventory for
701 downtown Nanjing where the monitoring sites were located. As large fractions of emissions
702 were allocated by the density of economy and population, however, the SO_2 emissions in the
703 regional emission inventory were estimated at 1791, 1721, 1918, and 1635 Mg at XWH, RJL,
704 ZHM and CCM sites, which were 4-5 times higher than those of our provincial inventory. In
705 MEIC, the emissions at XWH, RJL, ZHM and MGQ sites were identically estimated at 1298
706 Mg from the downscaling approach, and they were also much larger than those in the

Atmos. Chem. Phys. Discuss., doi:10.5194/acp-2016-567, 2016
Manuscript under review for journal Atmos. Chem. Phys.
Published: 25 July 2016

provincial inventory. Given the unfavorable condition of pollutant transport for 9th-10th October, the overestimation in local emissions around the downtown monitoring sites in the national and regional inventories thus lead to terribly high simulated concentrations, while the results using the provincial one were much more reasonable. The comparison confirmed the benefits of precise quantification of emissions on local air quality modeling.

Despite of significant improvement, overestimation in SO_2 concentrations still existed in the simulation with our provincial inventory, attributed possibly to the error of meteorology modeling. Here we selected XWH site as an example to conduct the back trajectory analysis using HYSPLIT model (http://ready.arl.noaa.gov/HYSPLIT.php). Shown in Figure S6 in the supplement, the air mass reaching the site at 50 m altitude came mainly from northeast at 11pm on 9th October. However, it was inconsistent with WRF modeling results, which indicated the dominating wind was from northwest (150°-170°) at that time. As mentioned above, a big power plant was located northwest to XWH (Figure 9a), and the site might partly be influenced by the large emissions from the plant and enhanced concentrations would then be obtained when northwest wind was simulated.

5 SENSITIVITY ANALYSIS OF $PM_{2.5}$ AND OZONE FORMATION IN NANJING

Using the improved provincial inventory, the sensitivity of $PM_{2.5}$ and O_3 concentrations to emissions were further analyzed through the Brute-Force method (BFM, Dunker et al., 1996). For $PM_{2.5}$, four simulation scenarios were designed: Scenario B (the base case) in which the emissions from all types of sources are included; and Scenarios S1, S2, and S3 in which the pollutant emissions of power, iron & steel and cement plants in D3 were zero out, respectively. The changes in simulated $PM_{2.5}$ ground concentrations in S1, S2, and S3 compared to those in base case for October 2012 are illustrated in Figure S7 in the supplement. The average concentration increments in urban area of Nanjing caused by power, iron &steel, and cement plants were calculated respectively at 3, 11 and 7 $\mu g/m^3$, accounting for 6%, 26% and 16% of the monthly mean $PM_{2.5}$ concentrations, and the maximum increments within the domain reached 10, 72, and 25 $\mu g/m^3$, respectively. Given the tiny emission fraction of power sector for primary $PM_{2.5}$ (4% in Jiangsu Province) and the small share in the ground layers

Atmos. Chem. Phys. Discuss., doi:10.5194/acp-2016-567, 2016
Manuscript under review for journal Atmos. Chem. Phys.
Published: 25 July 2016

Atmospheric Chemistry and Physics Discussions

(15% for 1st plus 2nd vertical layers), its contribution to $PM_{2.5}$ ground concentration was notably lower than those of iron & steel and cement. Summarized in Table 4 are the contributions of power, iron & steel, cement sectors to monthly mean $PM_{2.5}$ at the nine monitoring sites in Nanjing, October 2012. The contributions of the three sectors to average $PM_{2.5}$ concentrations at all the sites were estimated at 8%, 13% and 9%, respectively. Since all the sites are located in the urban or suburban areas, the estimated $PM_{2.5}$ contributions at individual site varied slightly to each other. Besides monthly mean, the hourly maximum and minimum contributions are provided as well in Table 4. The largest hourly contributions from power, iron & steel and cement plants to $PM_{2.5}$ concentrations were 65% at PKS, 89% at MGQ and 58% at both CCM and OCS, respectively. The contributions became negative at 2 pm on 26th October with average $PM_{2.5}$ concentration of all the sites observed as 164 $\mu g/m^3$ and simulated as 151 $\mu g/m^3$ under the base case, i.e., increased particle concentrations were simulated at the moment when emissions from given sector was turned off. The result indicated, on one hand, the relatively high uncertainty of simulation for heavy PM pollution episode dominated by regional transport. On the other hand, as the simulated increments were mostly from the elevated sulfate (SO_4^{2-}), nitrate (NO_3^-) and ammonium (NH_4^+), the negative contributions might also be caused by the complex chemical mechanisms of SO_2 and NOx reactions with NH_3 under the NH_3-rich condition in YRD (Wang et al., 2011). Intensive real-time observation on chemical composition of $PM_{2.5}$ is thus recommended to better capture and analyze the process.

To explore the sensitivity of O_3 formation to its precursor emissions, two scenarios were set besides the base case: the VOC-abatement scenario with 50% reduction of all anthropogenic VOCs emissions in D3 (Scenario P1), and the NOx-abatement scenario with 50% reduction of NOx in D3 (Scenario P2). Shown in Figure S8 in the supplement were the average O_3 concentration changes from October 6th to October 15th. The simulated O_3 average concentration from 11am to 5pm declined significantly under Scenario P1, with the maximum reduction at 54 $\mu g/m^3$ (Figure S8a) within D3, and changes in the downwind region were greater than the upwind. In contrast, the concentrations were generally enhanced under P2 with the maximum increment at 19 $\mu g/m^3$. Similar variation pattern was found for 1-hour maximum O_3 concentration in Figure S8b and monthly mean concentration in Figure S8c.

Atmos. Chem. Phys. Discuss., doi:10.5194/acp-2016-567, 2016
Manuscript under review for journal Atmos. Chem. Phys.
Published: 25 July 2016

Atmospheric Chemistry and Physics Discussions

766 The 1-hour maximum O_3 concentrations in most downwind area of Shanghai and southern
767 Jiangsu decreased 10-20 μg/m^3 with the reduction in VOCs emissions, and the concentrations
768 would generally increase 10-30 μg/m^3 with the NO_X reduction. The similar patterns of O_3
769 concentration variation in urban and downwind areas in D3 under P1 or P2 scenario indicated
770 that the O_3 formation was VOCs-limited in all those areas in southern Jiangsu. Therefore,
771 VOC emission abatement could be effective for O_3 pollution control in southern Jiangsu,
772 while NO_X abatement might aggravate the pollution in autumn.

773 The temporal changes in the simulated O_3 concentrations between the P1/P2 and base
774 scenarios at urban (XWH, SXL, RJL, MGQ, ZHM and CCM) and suburban sites (XLS, OCS
775 and PKS) in Nanjing were illustrated for October 6th-16th in Figure 10. Simulated O_3
776 concentrations at urban and suburban sites were generally decreased once the VOC emissions
777 declined and the maximum hourly reduction reached 77.3 and 49.6 μg/m^3, respectively. In
778 contrast, concentrations were elevated with the NOx emission reduction and the maximum
779 growth were 78.7 and 15.4 μg/m^3, respectively. Under VOCs-limited regime, in general, the
780 O_3 concentration would be little sensitive to the changes in NOx unless it was rich enough to
781 turn to the negative correlation with O_3. Therefore, due to the intensive NOx emissions from
782 on-road transportation in downtown Nanjing, the variations of O_3 concentrations in P2
783 scenario at urban monitoring sites were notably greater than those at suburban sites.
784

785 **6 CONCLUSIONS**

786 The bottom-up approach was applied to develop a high-resolution emission inventory for
787 Jiangsu, with substantial detailed information on local sources incorporated. Key parameters
788 relevant to emission estimation were examined and revised plant by plant including
789 geographic position, energy consumption and removal efficiencies of APCDs from various
790 data sources and on-site survey on large emitters. Compared to previous studies, the emission
791 fractions of point sources were significantly enhanced, except for NH_3 and OC, which are
792 mainly from agriculture activities and biomass open burning, respectively. As lower removal
793 efficiencies of dust collectors were obtained from local investigation, larger primary PM
794 emissions were estimated in our provincial inventory than other national or regional ones.

Atmos. Chem. Phys. Discuss., doi:10.5194/acp-2016-567, 2016
Manuscript under review for journal Atmos. Chem. Phys.
Published: 25 July 2016

Atmospheric Chemistry and Physics Discussions

795 Moreover, clear discrepancy existed in spatial distribution of industrial $PM_{2.5}$ emissions
796 between this work and the national inventory MEIC, indicating the uncertainty of emission
797 downscaling from coarse horizontal resolution. The spatial distribution of NO_X emissions in
798 the provincial inventory was more consistent with summer tropospheric NO_2 VCDs observed
799 from OMI than that of MEIC, particularly for the emissions from small and medium industrial
800 plants. WRF-CMAQ air quality modeling system was set up to evaluate the reliability and
801 improvement of the provincial emission inventory by comparing the simulation performance
802 with that using a national (MEIC) and regional one. Among the three inventories, the best
803 agreement was found between the observation and simulation with the provincial one for all
804 the concerned species at the nine monitoring sites in Nanjing, while underestimation existed
805 particularly for $PM_{2.5}$ and O_3 that were strongly influenced by secondary formation. Under the
806 unfavorable meteorology of pollutant transport, extremely high SO_2 concentrations were
807 simulated using the regional and national inventories, while the results using provincial one
808 were much closer to the observation. The results indicated the advantage of improved
809 estimation and spatial distribution of emissions on air quality modeling at regional or local
810 scales. The improved provincial inventory was further applied for the sensitivity analysis on
811 $PM_{2.5}$ and O_3 formation using BFM simulation, and provided the preliminary results for the
812 policy making of regional haze and photochemical pollution control in southern Jiangsu.
813 Limitations remained in the current inventory. Attributed to unavailability of detailed
814 information, the weekly and hourly variations of emissions could not be fully tracked for each
815 city, and the vertical distribution of emissions by sector, depending mainly on the stack height,
816 temperature and flow of flue gas, could not be accurately determined. Instead, empirical data
817 from previous work (Li et al., 2011; L. Wang et al., 2010; 2014) had to be applied, which
818 might be inconsistent with the reality. In addition, some sources were not included in the
819 current inventory, e.g., fugitive dust emissions from construction sites and road transportation,
820 resulting from lack of reliable data and thereby potentially large uncertainties in the emission
821 estimation at provincial level. Finally, the effects of source profiles on air quality modeling,
822 e.g., the speciation of primary $PM_{2.5}$ and VOC, were not evaluated. As they are important on
823 the formation of O_3 and secondary particles, more investigations on typical sources and
824 evaluation through chemistry transport modeling are suggested in the future.

Atmos. Chem. Phys. Discuss., doi:10.5194/acp-2016-567, 2016
Manuscript under review for journal Atmos. Chem. Phys.
Published: 25 July 2016

Atmospheric Chemistry and Physics Discussions

ACKNOWLEDGEMENT

This work was sponsored by the Natural Science Foundation of China (41575142), Natural Science Foundation of Jiangsu (BK20140020), Jiangsu Science and Technology Support Program (SBE2014070918), and Special Research Program of Environmental Protection for Commonweal (201509004). We would like to acknowledge Litao Wang from Hebei University of Engineering, Jia Xing from Tsinghua University for the assistance in CMAQ model, and Xiao Fu from Tsinghua University for providing the emission inventory for Yangtze River Delta region, China.

REFERENCES

Baker: Meteorological modeling protocol for application to $PM_{2.5}$/haze/ozone modeling projects, 2004.

Bo, Y., Cai, H., Xie, S. D.: Spatial and temporal variation of historical anthropogenic NMVOCs emission inventories in China, Atmos. Chem. Phys., 23, 7297-7316, 2008.

Boersma, K. F., Eskes, H. J., Dirksen, R. J., van der A, R. J., Veefkind, J. P., Stammes, P., Huijnen, V., Kleipool, Q. L., Sneep, M., Claas, J., Leitão, J., Richter, A., Zhou, Y., and Brunner, D.: An improved tropospheric NO2 column retrieval algorithm for the Ozone Monitoring Instrument, Atmos. Meas. Tech., 4, 1905–1928, doi:10.5194/amt-4-1905-2011, 2011.

Cai, H., Xie, S. D.: Estimation of vehicular emission inventories in China from 1980 to 2005, Atmos. Environ., 41, 8963-8979, 2007.

Cheng, Z., Chen, C. H., Huang, C., Huang, H. Y., Li, L., Wang, H. L.: Trans-boundary. primary air pollution between cities in the Yangtze River Delta. Acta Sci. Circum., 31, 686-694, 2011 (in Chinese).

Dong, Y. Q., Chen, C. H., Huang, C., Wang, H. L., Li, L., Dai, P., Jia, J. H.: Anthropogenic emissions and distribution of ammonia in Yangtze River Delta, Acta Sci. Circum., 29, 1611-1617, 2009 (in Chinese).

Dunker, A. M., Morris, R. E., Pollack, A. K., Schleyer, C. H., and Yarwood, G.: Photochemical modeling of the impact of fuels and vehicles on urban ozone using auto oil program data, Environ. Sci. Technol., 30, 787–801, 1996.

EEA (European Environment Agency): COPERT 4-Computer Programme to Calculate Emissions from Road Transport, User Manual (Version 9.0), Copenhagen, Denmark, 2012.

858 EEA (European Environment Agency): EMAP/CORINAIR Emission Inventory
859 Guidebook-2013, http://www.eea.euopa.eu//publications/emep-eea-guidebook-2013, 2013.

860 Emery, C., Tai, E., Yarwood, G.: Enhanced meteorological modeling and performance
861 evaluation for two Texas episodes, Report to the Texas Natural Resources Conservation
862 Commission, prepared by ENVIRON, International Corp, Novato, CA, 2001.

863 Fu, M. L., Ge, Y. S., Tan, J. W., Zeng, T., Liang, B.: Characteristics of typical non-road
864 machinery emissions in China by using portable emission measurement system, Sci. Total
865 Environ., 437, 255-261, 2012.

866 Fu, Q. Y.: Emission inventory and the foundation mechanism of high pollution of fine
867 particulate matters in Shanghai (in Chinese), Ph. D thesis, Fudan University, Shanghai, China,
868 2009.

869 Fu, X., Wang, S. X., Zhao, B., Xing, J., Cheng, Z., Liu, H., and Hao, J. M.: Emission
870 inventory of primary pollutants and chemical speciation in 2010 for the Yangtze River Delta
871 region, China, Atmos. Environ., 70, 39-50, 2013.

872 Han, K. M., Lee, S., Chang, L. S., and Song, C. H.: A comparison study between
873 CMAQ-simulated and OMI-retrieved NO_2 columns over East Asia for evaluation of NOx
874 emission fluxes of INTEX-B, CAPSS, and REAS inventories, Atmos. Chem. Phys., 15,
875 1913-1938, doi:10.5194/acp-15-1913-2015, 2015.

876 He, K. B.: Multi-resolution Emission Inventory for China (MEIC): model framework and
877 1990–2010 anthropogenic emissions, International Global Atmospheric Chemistry
878 Conference, 17–21 September, Beijing, China, 2012.

879 He, K. B. (eds): Guidebook of Air Pollutant Emission Inventory Development for Chinese
880 Cities, Beijing, 2015 (in Chinese).

881 He, L. Q., Hu, J. N., Zu, L., Song, J. J., Chen, D.: Emission characteristics of exhaust $PM_{2.5}$
882 and its carbonaceous components from China I to China III heavy-duty diesel vehicles, Acta
883 Scientiae Circumstantiae, 35, 656-662, 2015 (in Chinese).

884 Huang, C., Chen, C. H., Li, L., Cheng, Z., Wang, H. L., Huang, H. Y., Streets, D. G., Wang,
885 Y. J., Zhang, G. F., and Chen, Y. R.: Emission inventory of anthropogenic air pollutants and
886 VOC species in the Yangtze River Delta region, China, Atmos. Chem. Phys., 11, 4105-4120,
887 2011.

888 Huang, R. J., Zhang, Y., Bozzetti, C., Ho, K. F., Cao, J. J., Han, Y., Daellenbach, K. R.,
889 Slowik, J. G., Platt, S. M., Canonaco, F., Zotter, P., Wolf, R., Pieber, S. M., Bruns, E. A.,
890 Crippa, M., Ciarelli, G., Piazzalunga, A., Schwikowski, M., Abbaszade, G., Schnelle- Kreis,
891 J., Zimmermann, R., An, Z., Szidat, S., Baltensperger, U., Haddad, I. E., and Prevot, A. S.:
892 High secondary aerosol contribution to particulate pollution during haze events in China,
893 Nature, 514, 218–222, 2014.

894 Huang, X., Song, Y., Li, M. M., Li, J. F., Huo, Q., Cai, X. H., Zhu, T., Hu, M., and Zhang, H.
895 S.: A high-resolution ammonia emission inventory in China Global Biogeochem, Cycles, 26:
896 GB1030, doi:10.1029/2011GB004161, 2012.

897 Huo, H., Wang, M., Zhang, X. L., He, K. B. Gong, H. M., Jiang, K. J., Jin, Y. F., Shi, Y. D., Yu
898 X.: Projection of energy use and greenhouse gas emissions by motor vehicles in China: Policy
899 options and impacts, Energ. Policy, 43: 37-48, 2012.

900 JSNBS (Jiangsu Bureau of Statistics): Statistical Yearbook of Jiangsu, Beijing, China
901 Statistics Press, 2011 (in Chinese).

902 JSNBS (Jiangsu Bureau of Statistics): Statistical Yearbook of Jiangsu, Beijing, China
903 Statistics Press, 2013 (in Chinese).

904 Kain, J.: The Kain-Fritsch convective parameterization: An update, J. Appl. Meteor., 43,
905 170-181, 2004.

906 Kurokawa, J., Ohara, T., Morikawa, T., Hanayama, S., Janssens-Maenhout, G., Fukui, T.,
907 Kawashima, K., and Akimoto, H.: Emissions of air pollutants and greenhouse gases over
908 Asian regions during 2000–2008: Regional Emission inventory in Asia (REAS) version 2,
909 Atmos. Chem. Phys., 13, 11019–11058, doi:10.5194/acp-13-11019-2013, 2013.

910 Lei, Y., Zhang, Q., Nielsen, C., He, K. B.: An inventory of primary air pollutants and CO_2
911 emissions from cement production in China, 1990-2020, Atmos. Environ., 45, 147-154, 2011.

912 Li, L., Chen, C. H., Fu, J. S., Huang, C., Streets, D. G., Huang, Y. H., Zhuang, G. F., Wang, J.
913 Y., Jang, C. J., Wang, H. L., Chen, Y. R., and Fu, M. J.: Air quality and emissions in the
914 Yangtze River Delta, China, Atmos. Chem. Phys., 11, 1621-1639,
915 doi:10.5194/acp-11-1621-2011, 2011.

916 Ministry of Environmental Protection (MEP): China National Ambient Air Quality Standards,
917 GB3095-2012, MEP, Beijing, China, 2012 (in Chinese).

918 Mijling, B., Vander, A. R. J., Zhang, Q. 2013. Regional nitrogen oxides emission trends in
919 East Asia observed from space. Atmos. Chem. Phys., 13: 12003-12012.

920 National Bureau of Statistics (NBS): China Statistical Yearbook 2013, China Statistics Press,
921 Beijing, 2013a (in Chinese).

922 National Bureau of Statistics (NBS): China Industry Economy Statistical Yearbook 2012,
923 China Statistics Press, Beijing, 2013b (in Chinese).

924 National Bureau of Statistics (NBS): China Energy Statistic Yearbook 2012, China Statistics
925 Press, Beijing, 2013c (in Chinese).

926 Ohara, T., Akimoto, H., Kurokawa, J., Horii, N., Yamaji, K., Yan, X., and Hayasaka, T.: An
927 Asian emission inventory of anthropogenic emission sources for the period 1980–2020,
928 Atmos. Chem. Phys., 7, 4419–4444, doi:10.5194/acp-7-4419-2007, 2007.

929 Price, C., Penner, J. and Prather, M.: NOx from lightning, Part I: Global distribution based on
930 lightning physics, J. Geophys. Res. Atmos., 102, D5, DOI: 10.1029/96JD03504, 1997.

931 Sindelarova, K., Granier, C., Bouarar, I., Guenther, A., Tilmes, S., Stavrakou, T., Müller, J.-F.,
932 Kuhn, U., Stefani, P., and Knorr, W.: Global dataset of biogenic VOC emissions calculated by
933 the MEGAN model over the last 30 years, Atmos. Chem. Phys. Discuss., 14, 10725-10788,

934 doi:10.5194/acpd-14-10725-2014, 2014.

935 Streets, D. G., Bond, T. C., Carmichael, G. R., Fernandes, S. D., Fu, Q., He, D., Klimont, Z.,
936 Nelson, S. M., Tsai, N. Y., Wang, M. Q., Woo, J.-H., and Yarber, K. F.: An inventory of
937 gaseous and primary aerosol emissions in Asia in the year 2000, J. Geophys. Res., 108, 8809,
938 doi:10.1029/2002JD003093, 2003.

939 Street, D. G., Fu, J. S., Jang, C. J., Hao, J. M., He, K. B., Tang, X. Y., Zhang, Y. H., Wang, Z.
940 F., Li, Z. P., Zhang, Q., Wang, L. T., Wang, B. Y., Yu, C.: Air quality during the 2008
941 Beijing Olympic Games, Atmos. Environ.,41, 480-492, 2007.

942 Tang, X. L., Zhang, Y., Yi, H. H., Ma J. Y., Pu L.: Development a detailed inventory
943 framework for estimating major pollutants emissions inventory for Yunnan Province, China,
944 Atmos. Environ., 57, 116-125, 2012.

945 Tian, H. Z., Liu, K. Y., Hao, J. M., Wang, Y., Gao, J. J., Qiu, P. P., and Zhu, C. Y.: Nitrogen
946 oxides emissions from thermal power plants in China: Current status and future predictions,
947 Environ. Sci. Technol., 47, 11350-11357, 2013.

948 Wang, K., Zhang, Y., Jang, C., Phillip, S., and Wang, B.Y.: Modeling intercontinental air
949 pollution transport over the trans-Pacific region in 2001 using the Community Multi scale Air
950 Quality modeling system, J. Geophys. Res. Atmos., 114, D04307,
951 doi:10.1029/2008JD010807, 2009.

952 Wang, Q. D., Huo, H., He, K. B., Yao, Z. L., Zhang, Q.: Characterization of vehicle driving
953 patterns and development of driving cycles in Chinese cities, Transportation research part D:
954 transport and environment, 13, 289-297, 2008.

955 Wang, S. X., Zhao, M., Xing, J., Wu, Y., Zhou, Y., Lei, Y., He, K. B., Fu, L. X., and Hao, J.
956 M.: Quantifying the air pollutants emission reduction during the 2008 Olympic Games in
957 Beijing, Environ. Sci. Technol., 44, 2490-2496, 2010.

958 Wang, S. X., Xing, J., Jang, C. J., Zhu, Y., Fu, J. S., Hao, J. M.: Impact assessment of
959 ammonia emissions on inorganic aerosols in east China using response surface modeling
960 technique, Environ. Sci. Technol., 45: 9293-9300, 2011.

961 Wang, L. T., Jang, C., Zhang, Y., Wang, K., Zhang, Q., Streets, D. G., Fu, C. J., Lei, Y.,
962 Schreifels, J., He, K. B., Hao, J. M., Lam, Y. F., Lin, J., Meskhidze, N., Voorhees S., Evarts
963 D., Phillips S.: Assessment of air quality benefits from national air pollution control policies
964 in China. Part II: Evaluation of air quality predictions and air quality benefits assessment.
965 Atmos. Environ., 44, 3449-3457, 2010.

966 Wang, L. T., Wei, Z., Yang, J., Zhang, Y., Zhang, F. F., Su, J., Meng, C. C., and Zhang, Q.:
967 The 2013 severe haze over southern Hebei, China: model evaluation, source apportionment,
968 and policy implications, Atmos. Chem. Phys., 14, 3151–3173, doi:10.5194/acp-14-3151-2014,
969 2014.

970 Wei, W., Wang, S. X., Chatani, S., Klimont, Z., Cofala, J., and Hao, J. M.: Emission and
971 speciation of non-methane volatile organic compounds from anthropogenic sources in China,
972 Atmos. Environ., 42, 4976–4988, 2008.

973 Xia, S. J., Zhao, Q. Y., Li, B., Shen, G. F.: Anthropogenic source VOCs emission inventory
974 of Jiangsu Province, Research of Environmental Sciences, 27, 120-126, 2014 (in Chinese).

975 Xia, Y. M., Zhao, Y., Nielsen, C. P.: The benefits of China's efforts in gaseous pollutant
976 control indicated by the bottom-up emissions and satellite observations, Atmos. Environ., 136,
977 43-53, 2016.

978 Xing, J., Zhang, Y., Wang, S. X., Liu, X. H., Cheng, S. H., Zhang, Q., Chen, Y. S., Streets, D.
979 G., Jang, C. J., Hao, J. M., Wang, W. X.: Modeling study on the air quality impacts from
980 emission reductions and atypical meteorological conditions during the 2008 Beijing Olympics,
981 Atmos. Environ., 45, 1786-1798, 2011.

982 Yang, F., Tan, J., Zhao, Q., Du Z., He, K., Ma, Y., Duan, F., Chen, G., and Zhao, Q.:
983 Characteristics of $PM_{2.5}$ speciation in representative megacities and across China, Atmos.
984 Chem. Phys., 11, 5207-5219, doi:10.5194/acp-11-5207-2011, 2011.

985 Ye, S. Q., Zheng, J. Y., Pan, Y. Y., Wang, S. S., Lu, Q., and Zhong, L. J.: Marine emission
986 inventory and its temporal and spatial characteristics in Guangdong Province, Acta Sci.
987 Circum., 34, 537–547, 2014 (in Chinese).

988 Yin, S. S., Zheng, J. Y., Zhang, L. J., and Zhong, L. J.: Anthropogenic ammonia emission
989 inventory and characteristic in the Pearl River Delta region, Environ. Sci., 31, 1146–1151,
990 2010 (in Chinese).

991 Yin, S. S., Zheng, J. Y., Lu, Q., Yuan, Z. B., Huang, Z. J., Zhong, L. J., Lin, H.: A refined
992 2010-based VOC emission inventory and its improvement on modeling regional ozone in the
993 Pearl River Delta Region, China, Sci. Total Environ., 514, 426-438, 2015.

994 Zhang, H. L., Li, J. Y., Ying, Q., Yu, J. Z., Wu, D., Cheng, Y., He, K. B., Jiang, J. K.: Source
995 apportionment of $PM_{2.5}$ nitrate and sulfate in China using a source-oriented chemical transport
996 model, Atmos. Environ., 62, 228-242, 2012.

997 Zhang, L. J., Zheng, J. Y., Yin, S. S., Peng, K., and Zhong, L. J.: Development of non-road
998 mobile source emission inventory for the Pearl River Delta region, Environ. Sci., 31, 886-891,
999 2010 (in Chinese).

1000 Zhang, Q., Streets, D. G., Carmichael, G. R., He, K., Huo, H., Kannari, A., Klimont, Z., Park,
1001 I., Reddy, S., Fu, J. S., Chen, D., Duan, L., Lei, Y., Wang, L., and Yao, Z.: Asian emissions in
1002 2006 for the NASA INTEX-B mission, Atmos. Chem. Phys., 9, 5131-5153,
1003 doi:10.5194/acp-9-5131-2009, 2009.

1004 Zhang, Y. and Carmichael, G. R.: The role of mineral aerosol in tropospheric chemistry in
1005 East Asia-a model study, J. Appl. Meteorol., 38, 353-366, 1999.

1006 Zhang, Y., Liu, P., Pun, B., Seigneur, C.: A comprehensive performance evaluation of
1007 MM5-CMAQ for the Summer 1999 Southern Oxidants Study episode-Part I: Evaluation
1008 protocols, databases, and meteorological predictions, Atmos. Environ., 40, 4825-4838, 2006.

1009 Zhang, Y., Wang, W., Wu, S.-Y. Wang, K., Minoura, H., Wang, Z. F.: Impacts of updated
1010 emission inventories on source apportionment of fine particle and ozone over the southeastern

U.S., Atmos. Environ., 88, 133-154, 2014.

Zhao, B., Wang, P., Ma, J. Z., Zhu, S., Pozzer, A., and Li, W.: A high-resolution emission inventory of primary pollutants for the Huabei region, China, Atmos. Chem. Phys., 12, 481-501, doi:10.5194/acp-12-481-2012, 2012.

Zhao, B., Wang, S. X., Dong, X. Y., Wang, J. D., Duan, L., Fu, X., Hao, J. M., and Fu, J. S.: Environmental effects of the recent emission changes in China: implications for particulate matter pollution and soil acidification, Environ. Res. Lett., 8, 24-31, 2013.

Zhao, Y., Wang, S.X., Duan, L., Lei, Y., Cao, P.F., and Hao, J.M.: Primary air pollutant emissions of coal-fired power plants in China: current status and future prediction. Atmos. Environ., 42, 8442-8452, 2008.

Zhao, Y., Wang, S. X., Nielsen, C. P., Li, X. H., and Hao, J. M.: Establishment of a database of emission factors for atmospheric pollutants from Chinese coal-fired power plants, Atmos. Environ., 44, 1515-1523, 2010.

Zhao, Y., Nielsen, C. P., McElroy, M. B., Zhang, L., and Zhang, J.: CO emissions in China: uncertainties and implications of improved energy efficiency and emission control, Atmos. Environ., 49, 103-113, 2012a.

Zhao, Y., Nielsen, C. P., and McElroy, M. B.: China's CO_2 emissions estimated from the bottom up: Recent trends, spatial distributions, and quantification of uncertainties, Atmos. Environ., 59, 214-223, 2012b.

Zhao, Y., Zhang, J., Nielsen, C. P.: The effects of recent control policies on trends in emissions of anthropogenic atmospheric pollutants and CO_2 in China, Atmos. Chem. Phys., 13, 487-508, 2013.

Zhao, Y., Qiu, L. P., Xu, R. Y., Xie, F. J., Zhang, Q., Yu, Y. Y., Nielsen, C. P., Qin, H. X., Wang, H. K., Wu, X. C., Li, W. Q., and Zhang, J.: Advantages of a city-scale emission inventory for urban air quality research and policy: the case of Nanjing, a typical industrial city in the Yangtze River Delta, China, Atmos. Chem. Phys., 15, 12623-12644, doi:10.5194/acp-15-12623-2015, 2015.

Zheng, J. Y., Zhang, L. J., Che, W. W., Zheng, Z., and Yin, S. S.: A highly resolved temporal and spatial air pollutant emission inventory for the Pearl River Delta region, China and its uncertainty assessment, Atmos. Environ., 43, 5112–5122, 2009.

Zheng, J. Y., Fu, F., Li, Z. C., Wang, S. S., Zhong, L. J.: Implementation and evaluation of uncertainty propagation using stochastic response surface method based on the CMAQ model, Acta Sci. Circum., 32, 1289-1298, 2012 (in Chinese).

Atmos. Chem. Phys. Discuss., doi:10.5194/acp-2016-567, 2016
Manuscript under review for journal Atmos. Chem. Phys.
Published: 25 July 2016

Atmospheric Chemistry and Physics Discussions

FIGURE CAPTIONS

Figure 1. Modeling domain and locations of 43 meteorological and 9 air quality monitoring sites.

Figure 2. Source contributions to total estimated emissions by species in Jiangsu 2012. Colors indicate the sectors and the shade patterns indicate the source type (point, mobile and area).

Figure 3. Comparison between the emissions estimated in this work and other studies for Jiangsu. A and B indicate the emissions without and with open biomass burning, respectively.

Figure 4. Spatial distributions (a-c) and linear regression (d) of certain pollutant emissions from typical sources estimated in our provincial inventory and MEIC. (a) SO_2 from power plant; (b) NOx from transportation; (c) $PM_{2.5}$ from industry. The black points indicate the locations of plants with $PM_{2.5}$ emissions larger than 10 Gg estimated in this work.

Figure 5. Spatial distributions of NO_2 VCDs observed by OMI in Jiangsu in 2010 (a) and 2012 (b), and those of Jiangsu's NOx emissions from MEIC (c) and our provincial inventory (d) at the resolution of $0.25^{\circ}\times0.25^{\circ}$. Linear regressions of gridded VCDs and emissions are illustrated for MEIC (e) and our provincial inventory (f).

Figure 6. Spatial distributions of the monthly means of simulated SO_2, NO_2, $PM_{2.5}$ and O_3 concentrations using the national, regional and provincial emission inventories for October 2012.

Figure 7. The differences in the monthly means of simulated SO_2, NO_2, $PM_{2.5}$ and O_3 concentrations using different emission inventories: (a) Provincial–national; (b) Regional–national; and (c) provincial–regional. The black star A and triangle B referred to the locations of grids with maximum SO_2 emissions in provincial and regional inventory.

Figure 8. The observed and simulated hourly SO_2 concentrations at 3-hour interval using the national, regional, and provincial inventories at XWH (a), RJL (b), and ZHM (c) from October 6^{th} to 13^{th}, 2012.

Figure 9. Spatial distributions of the estimated SO_2 emissions in Nanjing at the resolution of 3×3km in the provincial (a), regional (b) and national emission inventory (c). The black dots indicate the locations of given air quality monitoring sites. The black star (point A) indicates the location of the power plant with the largest SO_2 emissions estimated in the provincial inventory. The black triangle (point B) indicates the speculated position of the same power plant in the regional inventory.

Figure 10. The changes in simulated O_3 concentrations at urban (XWH, SXL, RJL, MGQ, ZHM, and CCM) and suburban air quality monitoring sites (XLS, OSC, and PKS) in Nanjing under P1 (a) and P2 (b) scenarios compared to the base case for 6^{th}-16^{th} October 2012.

Atmos. Chem. Phys. Discuss., doi:10.5194/acp-2016-567, 2016
Manuscript under review for journal Atmos. Chem. Phys.
Published: 25 July 2016

Atmospheric Chemistry and Physics Discussions

TABLES

Table 1. The estimated annual emissions by city for Jiangsu 2012 (unit: million metric tons (Tg) for CO_2 and kilo metric tons (Gg) for other species).

City	SO_2	NOx	CO	TSP	PM_{10}	$PM_{2.5}$	BC	OC	CO_2	NH_3	VOCs
Southern											
Nanjing	140.6	210.5	742.9	157.3	97.3	75.8	5.8	7.1	97.1	64.2	221.9
Suzhou	220.8	286.7	1383.3	380.6	194.9	137.3	9.8	11.0	184.4	144.8	297.8
Wuxi	107.7	180.0	545.5	271.3	126.9	77.2	3.4	9.6	84.5	24.2	167.2
Changzhou	104.0	107.7	734.6	413.3	194.6	126.2	3.6	7.5	65.2	33.4	104.2
Zhenjiang	44.0	89.6	231.6	143.3	66.8	40.9	1.9	6.6	53.0	38.1	55.4
Central											
Nantong	76.8	130.1	443.4	244.9	108.2	66.0	4.8	9.3	51.6	181.7	162.2
Yangzhou	55.3	93.9	310.7	54.1	39.9	31.1	2.6	8.5	52.1	83.1	82.5
Taizhou	56.6	70.5	315.1	207.6	98.2	52.3	2.7	8.8	31.4	100.7	76.9
Northen											
Xuzhou	138.9	232.5	805.5	223.2	146.5	101.9	6.1	19.1	139.2	49.2	161.2
Huai'an	52.2	61.5	590.0	97.4	64.5	49.5	3.7	12.0	32.5	195.9	78.6
Yancheng	49.9	78.5	639.7	203.8	111.8	72.0	5.6	16.1	28.2	101.0	185.0
Lianyungang	60.6	61.0	571.1	131.0	89.0	68.6	3.9	11.9	28.3	25.1	78.0
Suqian	34.1	39.7	366.8	77.8	55.5	42.3	3.2	11.0	12.9	59.1	76.4
Total	1141.5	1642.2	7680.0	2605.6	1394.0	941.1	57.0	138.5	860.5	1100.3	1747.3

Atmos. Chem. Phys. Discuss., doi:10.5194/acp-2016-567, 2016
Manuscript under review for journal Atmos. Chem. Phys.
Published: 25 July 2016

Atmospheric Chemistry and Physics Discussions

Table 2. Model performance statistics for concentrations of given species from observation and CMAQ simulation using the national, regional and provincial inventories at the nine air quality monitoring sites in Nanjing for October 2012.

Pollutants	National (MEIC)		Regional (Fu et al., 2013)		Provincial (this work)	
	NMB	NME	NMB	NME	NMB	NME
SO_2	48.45%	76.53%	74.08%	95.04%	-9.97%	47.49%
NO_2	21.02%	35.99%	29.84%	43.45%	-14.47%	33.22%
O_3	-65.55%	68.57%	-53.93%	61.59%	-24.98%	44.29%
$PM_{2.5}$	-51.63%	55.32%	-49.16%	56.00%	-43.64%	51.81%

Note: NMB and NME were calculated using following equations (P and O indicate the results from modeling prediction and observation, respectively):

$$NMB = \frac{\sum_{i=1}^{n}(P_i - O_i)}{\sum_{i=1}^{n} O_i} \times 100\%; \quad NME = \frac{\sum_{i=1}^{n}|P_i - O_i|}{\sum_{i=1}^{n} O_i} \times 100\%$$

Atmos. Chem. Phys. Discuss., doi:10.5194/acp-2016-567, 2016
Manuscript under review for journal Atmos. Chem. Phys.
Published: 25 July 2016

Atmospheric Chemistry and Physics Discussions

Table 3. The annual SO_2 emissions estimated in three inventories at given air quality monitoring sites in downtown Nanjing.

SO_2/Mg	National (MEIC)	Regional (Fu et al., 2013)	Provincial (this work)
XWH	1297.5	1790.9	411.0
RJL	1297.5	1720.8	303.1
ZHM	1297.5	1918.3	396.2
CCM	928.6	1635.3	371.8
MGQ	1297.5	478.6	395.0

Atmos. Chem. Phys. Discuss., doi:10.5194/acp-2016-567, 2016
Manuscript under review for journal Atmos. Chem. Phys.
Published: 25 July 2016

Atmospheric Chemistry and Physics Discussions

Table 4. The monthly mean contributions of power, iron & steel and cement plants to the $PM_{2.5}$ concentrations at the air quality monitoring sites in Nanjing in October 2012.

Monitoring site	Contri. of power (%)			Contri. of iron & steel (%)			Contri. of cement (%)		
	Max.	Min.	Ave.	Max.	Min.	Ave.	Max.	Min.	Ave.
XWH/SXL	52	-6	8	82	-2	14	43	-1	8
RJL	42	-6	7	79	0	11	44	0	9
ZHM	44	-5	7	71	-3	12	48	0	9
CCM	32	-8	7	83	-4	13	58	-5	8
MGQ	58	-5	9	89	-2	8	35	-5	7
XLS	35	-5	7	67	-3	10	57	0	10
PKS	65	-6	7	77	-1	11	45	-1	7
OCS	33	-7	7	87	0	12	58	0	8

Note: Max., min., ave. and contri. indicate maximum, minimum, average and contribution, respectively.

Atmos. Chem. Phys. Discuss., doi:10.5194/acp-2016-567, 2016
Manuscript under review for journal Atmos. Chem. Phys.
Published: 25 July 2016

Atmospheric Chemistry and Physics Discussions

Figure 1

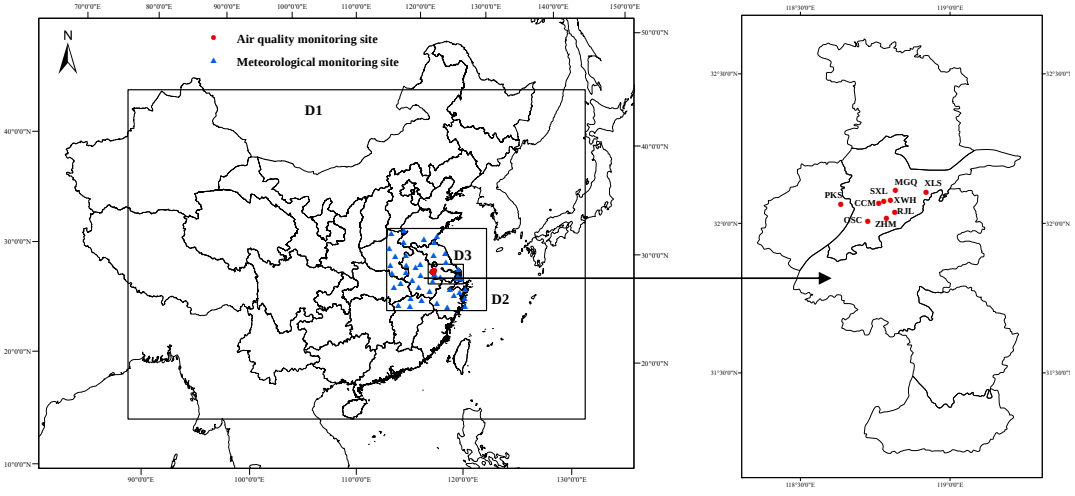

Atmos. Chem. Phys. Discuss., doi:10.5194/acp-2016-567, 2016
Manuscript under review for journal Atmos. Chem. Phys.
Published: 25 July 2016

Atmospheric Chemistry and Physics Discussions

Figure 2

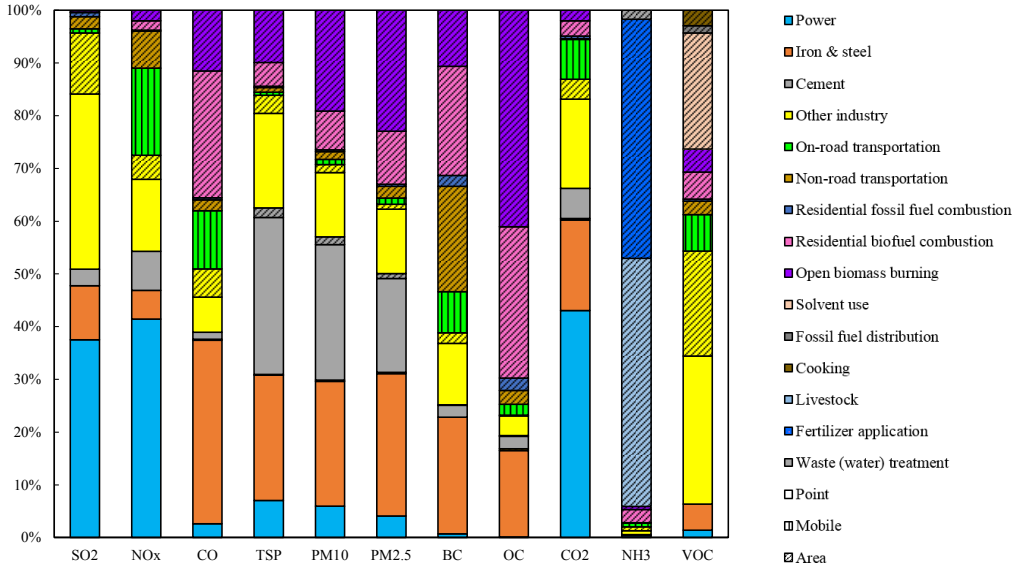

Atmos. Chem. Phys. Discuss., doi:10.5194/acp-2016-567, 2016
Manuscript under review for journal Atmos. Chem. Phys.
Published: 25 July 2016

Atmospheric Chemistry and Physics Discussions

Figure 3

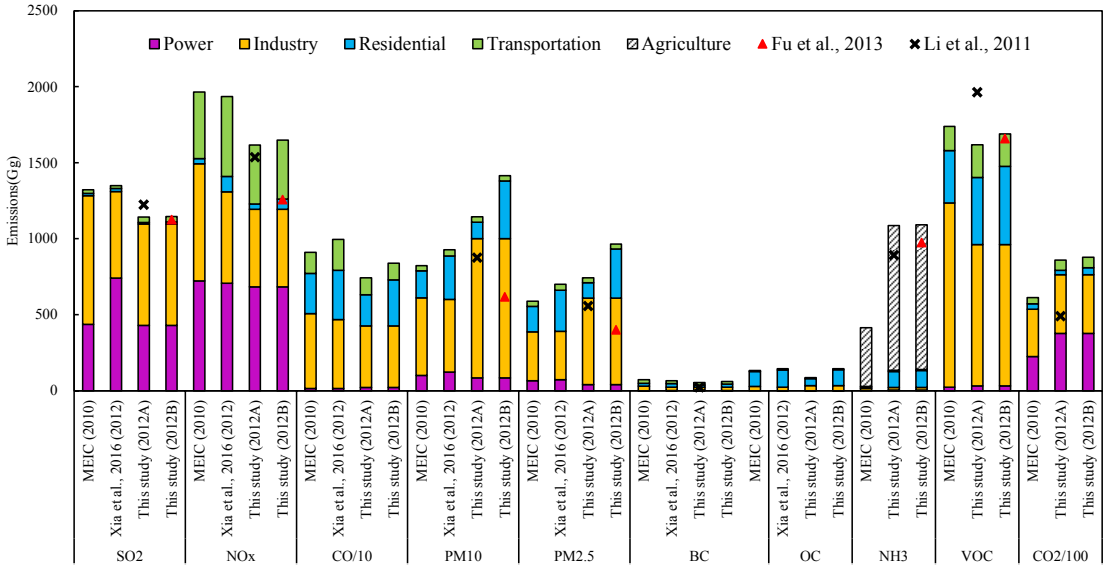

Atmos. Chem. Phys. Discuss., doi:10.5194/acp-2016-567, 2016
Manuscript under review for journal Atmos. Chem. Phys.
Published: 25 July 2016

Atmospheric Chemistry and Physics Discussions

Figure 4

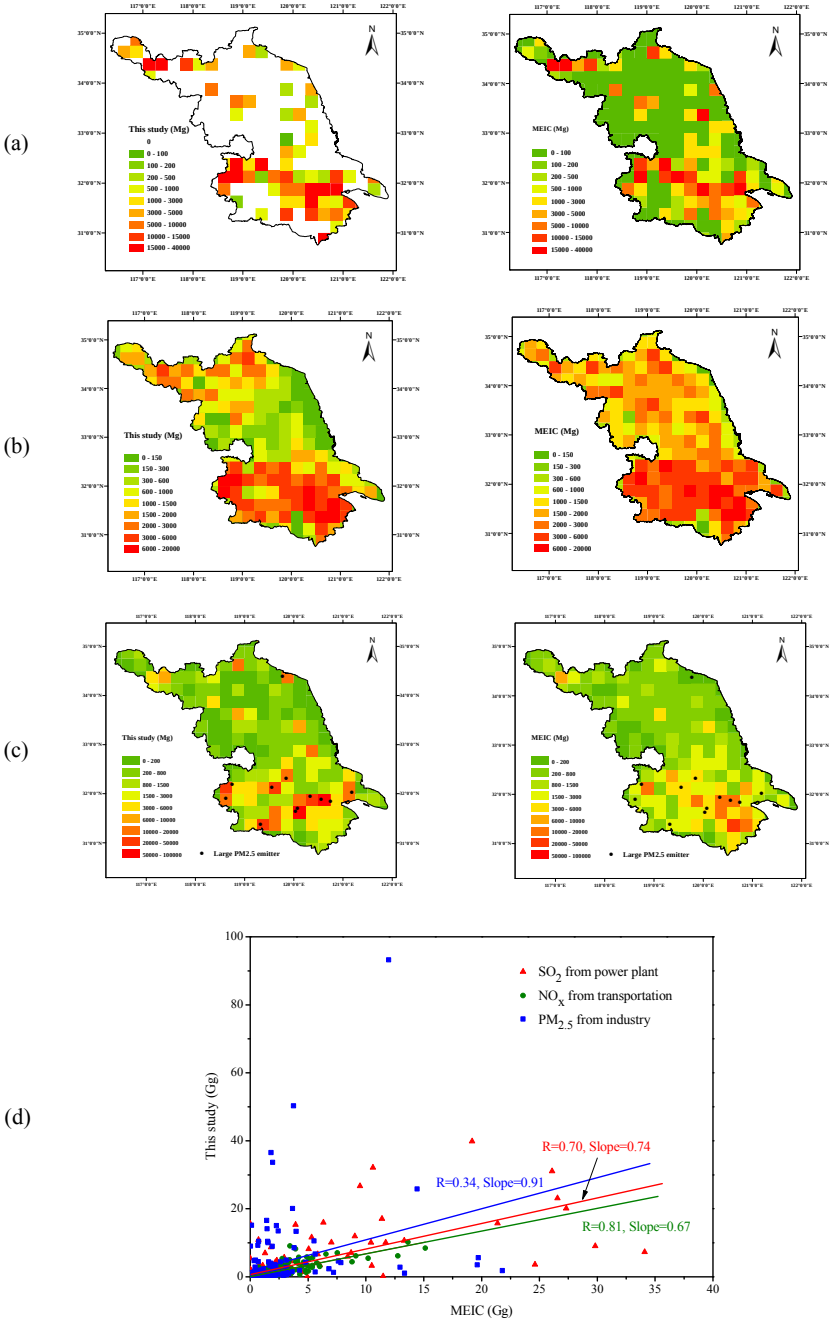

Atmos. Chem. Phys. Discuss., doi:10.5194/acp-2016-567, 2016
Manuscript under review for journal Atmos. Chem. Phys.
Published: 25 July 2016

Atmospheric Chemistry and Physics Discussions

Figure 5

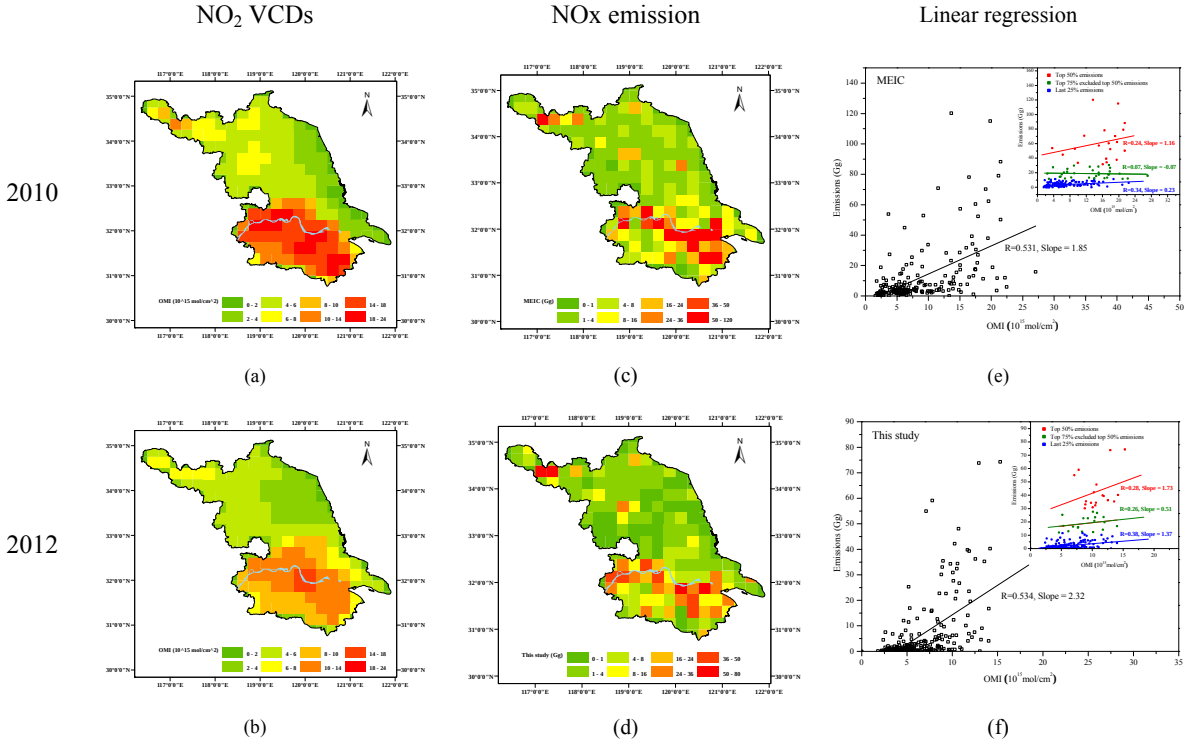

Atmos. Chem. Phys. Discuss., doi:10.5194/acp-2016-567, 2016
Manuscript under review for journal Atmos. Chem. Phys.
Published: 25 July 2016

Atmospheric Chemistry and Physics Discussions

Figure 6

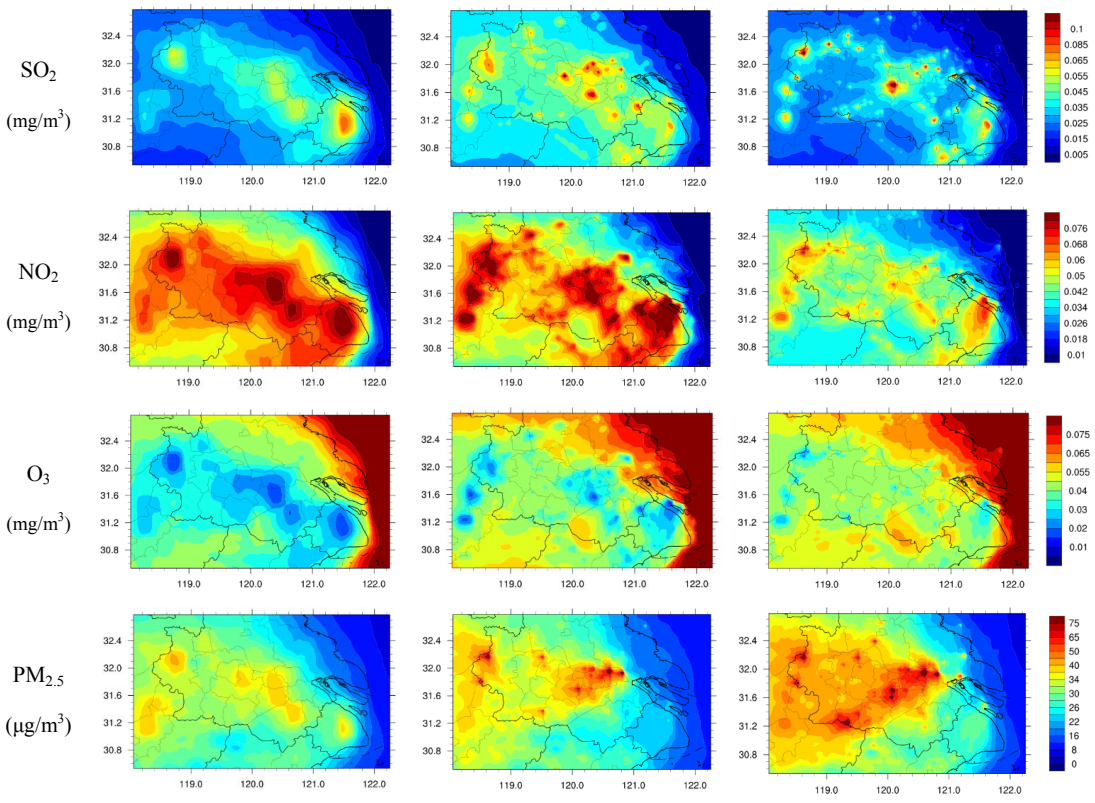

(a) National (MEIC) (b) Regional (Fu et al., 2013) (c) Provincial (this work)

Atmos. Chem. Phys. Discuss., doi:10.5194/acp-2016-567, 2016
Manuscript under review for journal Atmos. Chem. Phys.
Published: 25 July 2016

Atmospheric Chemistry and Physics Discussions

Figure 7

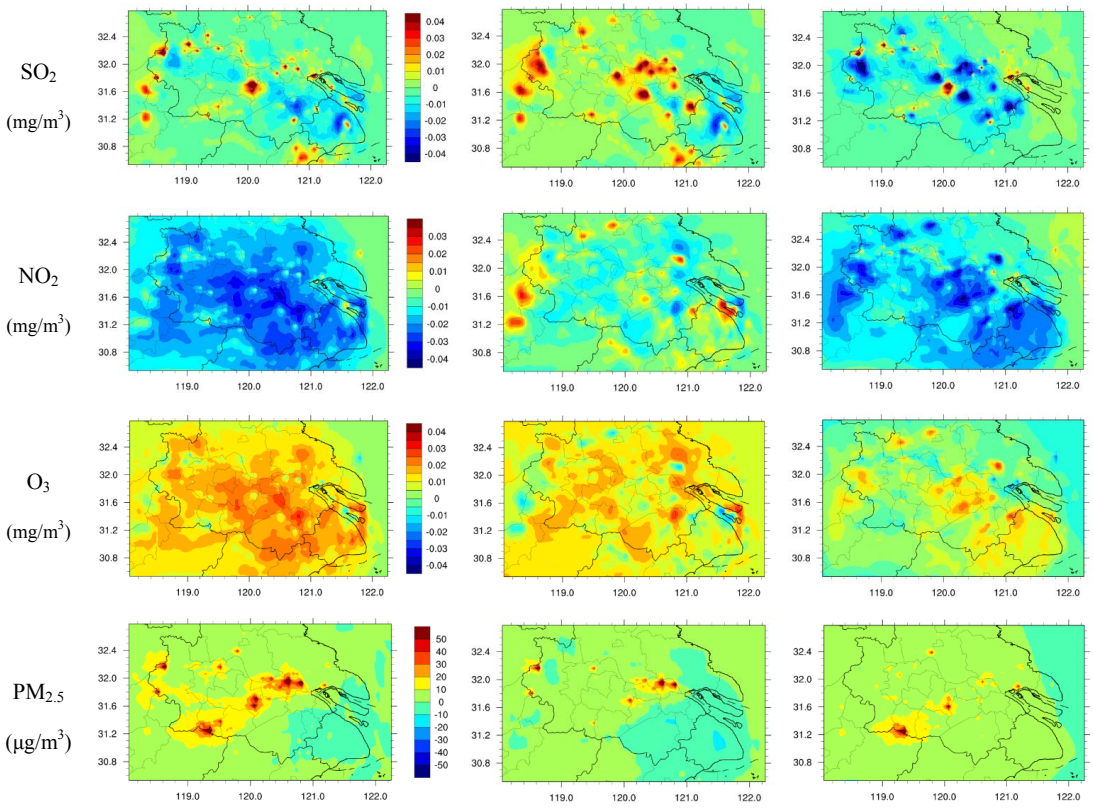

(a) Provincial – national (b) Regional – national (c) Provincial – regional

Atmos. Chem. Phys. Discuss., doi:10.5194/acp-2016-567, 2016
Manuscript under review for journal Atmos. Chem. Phys.
Published: 25 July 2016

Atmospheric Chemistry and Physics Discussions

Figure 8

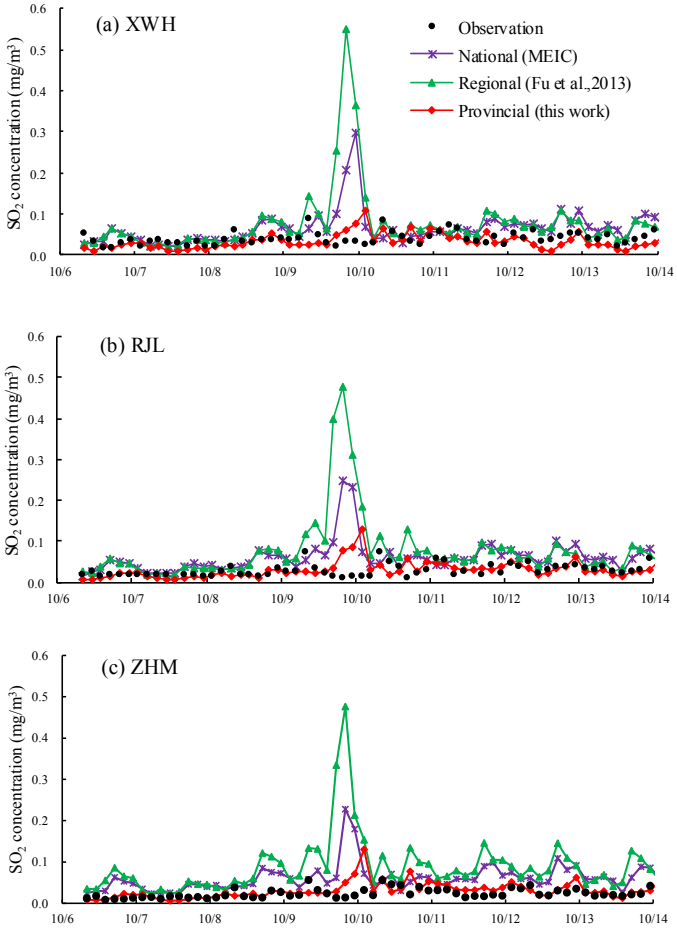

Atmos. Chem. Phys. Discuss., doi:10.5194/acp-2016-567, 2016
Manuscript under review for journal Atmos. Chem. Phys.
Published: 25 July 2016

Atmospheric Chemistry and Physics Discussions

Figure 9

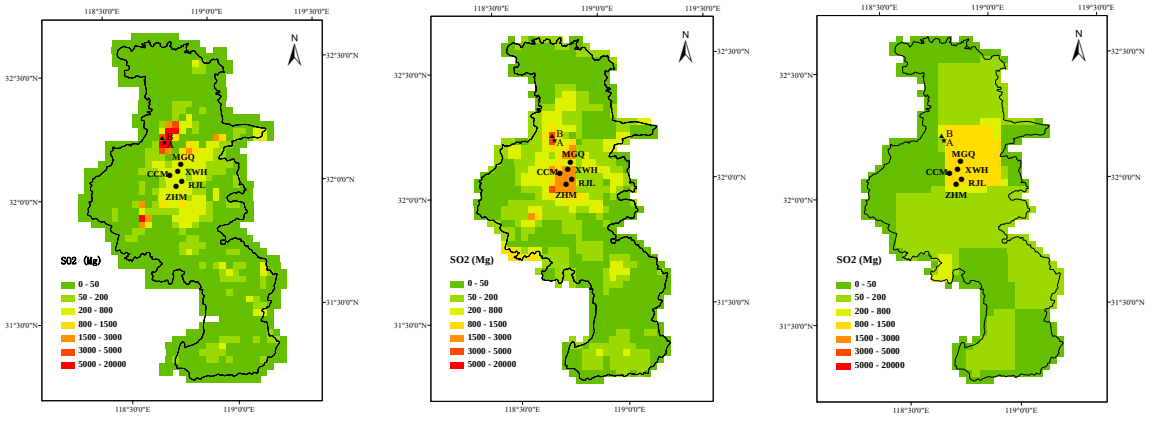

(a) (b) (c)

Atmos. Chem. Phys. Discuss., doi:10.5194/acp-2016-567, 2016
Manuscript under review for journal Atmos. Chem. Phys.
Published: 25 July 2016

Atmospheric Chemistry and Physics Discussions

Figure 10

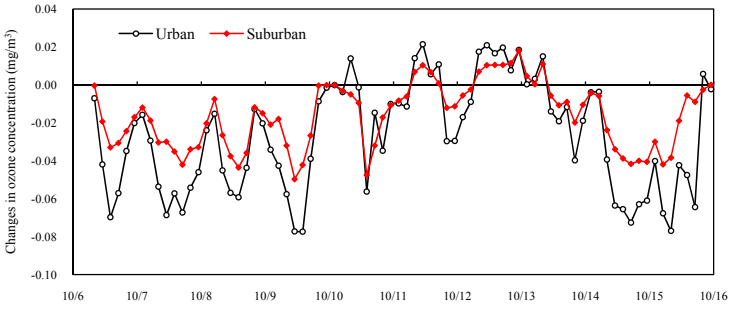

(a)

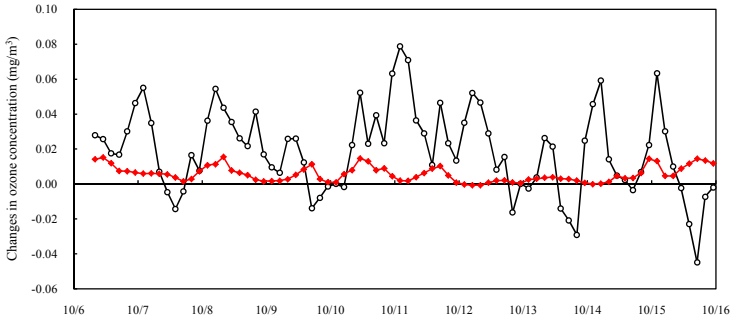

(b)